PATTERNED POLYMER FILMS USING SOFT-LITHOGRAPHY & MICRO MOLDING IN CAPILARIES (MIMIC)

A Dissertation

by

Afia Asif

Submitted to the

Graduate School of Engineering & Science
In Partial Fulfillment of the Requirements for
the Degree of

Masters of Science

in the
Department of Electrical and Electronics Engineering

Özyeğin University
May, 2017

THESIS APPROVAL FORM

Approved by:

Asst. Professor. Dr. Ahmet Tekin,
Advisor,
Department of Electrical and
Electronics Engineering
Özyeğin University

Assoc. Professor, Dr. M. Serdar Onses,
Committee Member,
Department of Materials Sciences &
Engineering
Erciyes University

Assoc. Professor, Dr. Goksenin
Yaralioglu, Committee Member,
Department of Electrical and
Electronics Engineering
Özyeğin University

Date Approved: 3rd May, 2017

ACKNOWLEDGEMENTS

This dissertation is the result of my Master's Degree research work which was accomplished in the Department of "Electrical and Electronics Engineering" of Graduate School of Istanbul Sehir University and Ozyegin University, Istanbul, Turkey from February 2015 to February 2017. The overall project was funded by Scientific and Technological Research Council of Turkey, named as "**TUBITAK**" under the grant nµmber 115M220, for year 2015-2017. This project was also in collaboration with Erciyes University.

First of all, I would like to thank my supervisors Dr. Serdar Onses from the Erciyes University, and Dr. Melikhan Tanyeri from Istanbul Sehir University for giving me an opportunity to work with this interesting project, which not only made me a better person in my research work but also taught me the technical depths related to my major "Nanotechnology". I would like to thank specially to Dr. Ahmet Tekin from Ozyegin University, who not only willingly accepted to be my supervisor after my transfer from Istanbul Sehir University to Ozyegin University, but also benefited me with his interesting ideas and keen motivation at every step for me to outperform and to particularly focus on

my publication from this research. I thank him for all the guidance and suggestions towards my work.

I thank Graduate School of Ozyegin University for support and massive encouragement during my one semester studies. I want to thank to the State Universities, “Bogazici University” and “Istanbul Technical University” for providing me the chance to use their expensive cleanroom facilities and to let me conduct my experiments for my research work. Also, I want to thank specially to my collaboration team in the “Erciyes University” under directions of Dr. Serdar Onses for giving me the best experience of collaboration and to support for developing my abilities to work in group teams. I learnt how beautifully the productivity to carry out work increases by collaboration in research projects. I want to thank my co-worker and officemate Muhammad Salman Khan for his entire support for lab work regarding to the project and for daily help.

Special thanks to the Thesis Defense Jury Members for their precious time to be a part of my thesis defense to judge and to listen to it and providing their feedbacks.

ABSTRACT

This research work is important because it reports a low cost method to pattern large area surfaces using soft-lithographic approach through several polymers, particularly with the self-assembly of block co-polymers (BCPs) and also by fabricating end-grafted polymer chains for selective immobilization and assembly of plasmonic nanoparticles (NPs). The demand for patterning large surface areas by patterning polymers is of quite interest because photo-lithograpghy makes it very expensive and complex. Patterning polymers approach in this work, relies on the capillary flow of polymers into the channels formed by an elastomeric mold and substrate, in a process called as micromolding in capillaries (MIMIC). P(S-b-pMMA) for BCPs, and hydrooxyl-terminated poly(2-vinylpyridine) (P2VP) and poly(ethylene glycol) (PEG) for polymer brushes are selectively deposited into linear features with the MIMIC process. BCPs self-assembly with the patterened features resulted in nanoscale structures over large surface arears. On the other hand, the localized grafting of the polymers through thermal annealing followed by washing leads to patterns of polymer brushes. The results show the ability to pattern polymer brushes with line widths as small as 1.5 μm at a height of ~3.5 nm (P2VP) and ~10 nm (PEG), and a length up to 0.5 cm. These patterns serve as localized binding sites for the specific and uniform immobilization of Au NPs with diameters of 20 nm and 60 nm. The immobilized Au NPs exhibited strong and localized surface enhanced Raman scattering effects from the patterned regions. The ability to pattern polymer

brushes and plasmonic NPs over large areas with a low-cost process may enable applications that range from molecular sensors to biotechnology. The low cost method to pattern large areas using BCP self-assembly through elastomeric PDMS molds would give boost to the solution of the commercialization of nano-patterns below ~20nm for semiconductor industries with an explicit ease of fabrication.

KEYWORDS: Blockcopolymers, polymer brushes, soft-lithography, nanoparticles, MIMIC, plasmonics

CHAPTER 1: INTRODUCTION

Self-assembly of block copolymers in thin films provide practical routes to dense nanoscale structures as a technologically viable patterning technique. Block copolymers are made up of blocks consisting of different structural units, which have different chemical properties and are covalently bonded to each other. Usually, block copolymers are formed with repeating units of polymers or "blocks" in a particular sequence. One of the simplest examples is the block copolymer named as SBS (Styrene Butatine Styrene) present in SBS rubber, used to produce tires for automobile vehicles. Some of the other applications involve block copolymers usage in light emitting diodes [1] and drug delivery systems [2].

Block copolymers play a vital role when it comes to serve as a material for patterning lithographic features. If partitioned, block copolymers can segregate into various sequences and can self-assemble them into mesoscopic lattice structures or features called as "micro or nano-domains" which can be periodic for different lengths.

The patterning attribute of block copolymers with different scales of dimensions are of great scientific and industrial interest. The continued demand of electronic instrµments and computational memory storage devices require further miniaturized and dense features to be implemented particularly in efficient and cost effective manner. Self-assembly of block copolymers contribute to this hope of stretching the boundaries of scaling down of

pattering techniques purpose by eliminating the barriers. Block copolymers exhibit the capability of large area patterning which has boosted up their utmost need for the technological and semiconductor industries.

We report a new method for fabrication of multiplex and hierarchical patterns with dimensions that span the scale of nanometers to centimeters, using patterned deposition of blockcopolymers (BCPs) films. This approach enables localized delivery of BCPs through a microfluidic (MF) molding method in short time scales (parallel processing) using elastomeric molds offering a low cost process. Longer BCPs nanopatterns over a large surface areas of substrates obtained from low cost method such as using PDMS molds can potentially replace the ultimate need for conventional lithography especially for applications in leading semi-conductor industries like IMEC and Intel. Here in this work, micro-patterns of diverse geometries were fabricated through conventional photo-lithography process with negative mask using SU-8 photoresist. Positive replicas of elastomeric stamps/molds were made of Poly (Dimethylsiloxane) PDMS which were obtained from negative mask using soft-lithography techniques. PDMS stamps were washed with DMF and were placed over a chemically treated substrate. BCPs of PS-PMMA solution was made with different concentrations and was poured at the one end of the channel. It was drawn into the micro channels with the effect of spontaneous capillary -flow process. It was further annealed at certain temperature to evaporate the solvent and for getting BCPs films deposited patterns in the channels.

Using thin films of BCPs and micro molding in capillaries (MIMIC) techniques, we are successfully able to guide the self-assembly of Block Copolymers on chemically patterned substrates with nanopatterns of dimensions as small as 50nm. Currently, two different

approaches that are (i) Microfluidic molding with controlled weights and (ii) effects of different Concentrations of BCPs would be explored for the patterned deposition of multiple BCPs on the same substrate to form self-assembled nanostructures with different dimensions and geometries. Lastly, we would focus on Nanoimprint Lithography and writing patterns with Electron beam lithography on topographically and chemically patterned substrates.

1.1 Background of Polymer Physics

Polymers are strongly essential and utilitarian in almost everywhere now a days in hµman life. Usually, when it comes to think about polymers, the first notion that comes in mind is the “wasteful”, “cheap”, and “unnatural” material which might seem not of much significance. The growth and development of polymers was firs initiated by the investigation of the polymers replacements for natural materials. Polymers these days have proved to be cheap substitutes for natural materials providing wide variety of applications. World’s plastic production is in billions of kilograms and plastic industry is fourth largest industry in United States [3]. Further improvements and breakthrough promotions are expected from polymers utilization for the growth of overall economy of the world.

Polymers are derived from petroleµm and because of their low cost attribute they are the source to provide the abundant stock for multiple uses. It is estimated that almost less than 5 barrels of petroleµm is enough to produce polymers and they are potentially in competition to produce thermoplastics and specialty polymers. Today, polymers are

produced in bulk quantity with a wide range of diversity in their variety and kinds. Some of the daily uses of polymers include, automobile body parts, aircraft parts (airframe and interiors), film packaging, insulation and sealing insulations, shoe soles, fibers for clothing and carpets, rubbers of tires for automobiles, paints, and foams serving various purposes.

1.1.1 Size of Polymer Molecules

A several models exist in order to define the polymer configuration. A model of polymer chain with random walk in three dimensional 3D can defined as the configuration of a linear, freely jointed and long chain of polymers. Out of several models, a model by Werner Kuhn, who developed the first model of the viscosity of polymer solutions by using statistical mechanics can be used to describe the polymer configuration. In three dimensions, a Gaussian coil with Radius of gyration $R_g = a\sqrt{\frac{1}{6}N}$, defines a maximµm entropy configuration for a polymer chain with length N units of steps a long, whereas, a is the Kuhn statistical length [4,5]. Other models also exist but will not be discussed here.

1.1.2 Polymer Dynamics

The physical and chemical configurations of the polymer chain is essential in relation to many processes and to end user properties. Polymer molecules are long and liner macromolecules made up of a large nµmber of chemical units or monomers, which are covalently bonded. For most polymers, these molecules form very long chains. Polymers are composed of basic structures called **"mer"** units. A molecule with just one "mer" is a monomer. When the polymer chain is in solution, in the melt or in the solid state, the shape can be considered as random coil configuration.

Several models have been developed in order to describe the mechanical and self-diffusion properties of polymer. Only two of the models are discussed below.

The Rouse model, which is applicable for short chain in the melt state, consist of a Gaussian worm-like chain which can exchange energy with its surroundings, and describe conformation by a contour function r(s,t) [6]. The equation of motion of the contour function is:

$$m\ddot{r} + \zeta \dot{r} - kr^n = \text{f (s,t)} \qquad (1.1)$$

ζ - friction coefficient due to surrounding mediµm.

$k = {}^{3k_B T}/_{a_r}$ due to Gaussian chain entropy.

f (s, t) - Langevin force due to thermal noise :

The principle results in chain center of mass diffusion coefficient.

$$D_{c.o.m} = {k_B T}/{\zeta N} \quad (1.2)$$

While, according to Zimm model, which is applicable to polymers in dilute solution, takes into account hydrodynamic drag force on polymer coil due to solvent. A force acting on polymer coil creates flow field with net component in the same direction as the primary force. Each particle creates a dragging force and these particles or beads in group make a polymer coil. Effective hydrodynamic radius of the coil is defined by:

$$R_h = {\zeta_p}/{6\pi\eta} \quad (1.3)$$

Friction coefficient of a polymer molecule is given as:

$$\zeta_p = 4\pi\eta R_g \rightarrow R_h \approx {2R_g}/{3} \quad (1.4)$$

Einstein Equation gives us:

$$D_{c.o.m} = {k_B T}/{4\pi\eta R_g} \rightarrow \mathrm{D} \propto N^{-0.6} \quad (1.5)$$

Polymers behave like colloidal particles, same pair distribution function as for a diffusing colloid:

$$g(r, t) = \left(\frac{1}{4\pi Dt}\right)^{3/2} \exp\left(\frac{-r^2}{4Dt}\right) \quad (1.6)$$

Other models also exist but will not be discussed here.

1.1.3 Glass Transition Temperature

By definition, glass temperature is one of the most important characteristic due to which mechanical properties of polymers such as viscosity and shear modulus changes because the polymer changes from hard or glassy state to a soft or rubbery material. Mechanically, the shear modulus of the hard polymer is on the order of 1 GPa for many of the polymers. But in glassy state, the motion happens due to vibrations or rotations of the molecules by keep the mass at the center of the molecule.

Near to the transition temperature, polymer softens and changes its state into rubber like material because of the drop in its shear modulus. Usually, the transition temperature is higher for the polymers which are hard and have glassy state [7].

1.2 Block Copolymers

In our study we are interested in specific type of polymers called as block copolymers. The simplest definition of block copolymers is that they are made up of blocks of different polymerized monomers, which have different chemical properties and are covalently bonded to each other. Every type of block copolymer has its own production protocol. Some of the configurations of types of block copolymers consist of (a) di-block (b) tri-block and (c) branched copolymers. **Fig.1** shows these symmetries.

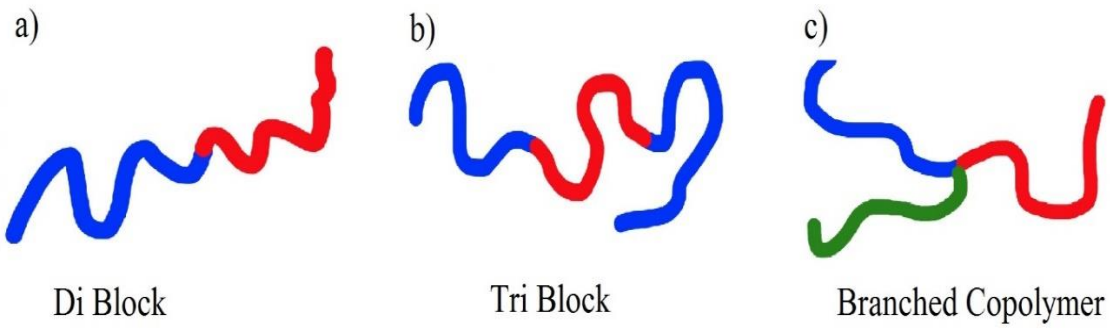

Fig 1. Different Symmetries of Block Copolymers. a) di-block, b) tri-block, c) branched Copolymer

1.2.1 Block Copolymers and Flory Huggins Theory

The covalent linkages between these individual blocks prevent macroscopic phase separation even when the polymer blocks are thermodynamically incompatible (G.E.S.Toombes) [8]. For simple understanding, a blend of two homopolymers i.e. X and Y, the interaction between X and Y homopolymers depend on the experimental parameters which are (i) The degree of polymerization (N), (ii) The composition (f), (iii) The Flory-Huggins interaction parameter. The Flory-Huggins equation affecting the free energy of a blend is as follows:

$$\frac{\Delta G_{mix}}{k_b T} = \frac{1}{N_A}\ln(f_A) + \frac{1}{N_B}\ln(f_B) + f_A f_B \chi \qquad (1.7)$$

In the third term of equation, χ is associated with the X-Y monomer contacts and is dependent on both temperature and chemistry of these molecules. While the first two terms

in equation corresponds to the configuratıonal entropy of the system (Segalman et.al, 2004)[9]. **Fig 2.** Shows the different phases for block co polymers self-assembly.

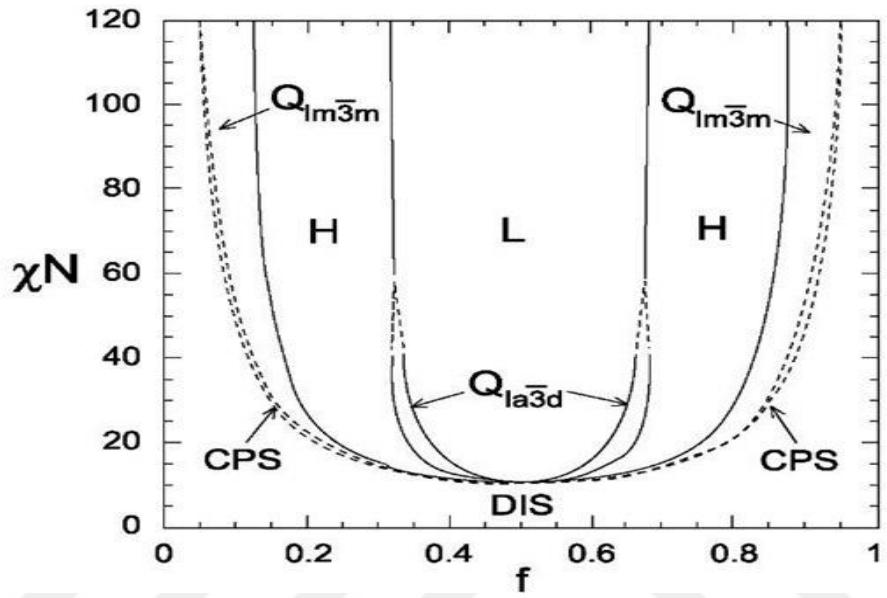

Fig 2. Phase Diagram of Self Assembly of Block Copolymers [8]

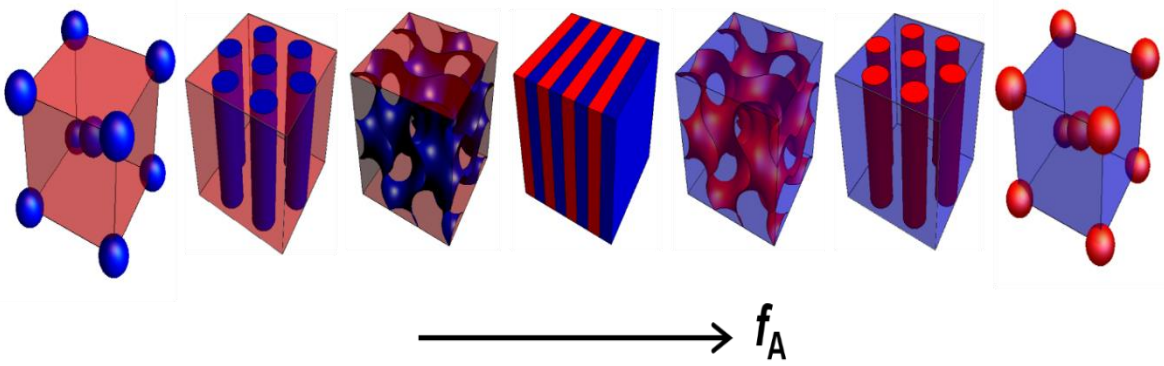

Fig 3. Orientation Structures Diagram of Self Assembly of Block Copolymers [8]

1.2.2 Block Copolymer Structures and Self Assembly

When block copolymers confined to a thin film, the substrate surface plays the crucial role in the orientations of the block copolymers domains. **Fig 3.** Shows different orientations in which block co polymers can self-assemble themselves on various environmental conditions. Block copolymer (BCP) self-assembly can spontaneously generate periodic arrays of micro-domains with versatile morphology and nanoscale feature size in the range of ca. 10–100 nm [10].

1.3 Applications of Block Copolymers

1.3.1 Block Copolymers Thin Films

Block copolymers have been considered one of the most promising techniques for many applications such as patterning, based on principle of their ability to form regular nanometer scale patterns over a well patterned substrate surface. Through BCPs, patterns of even smaller dimensions especially in length scales can be achieved easily which many other conventional lithographic techniques cannot provide. **Fig 4 e**xhibits the BCP thin films self-assembly structures as follows:

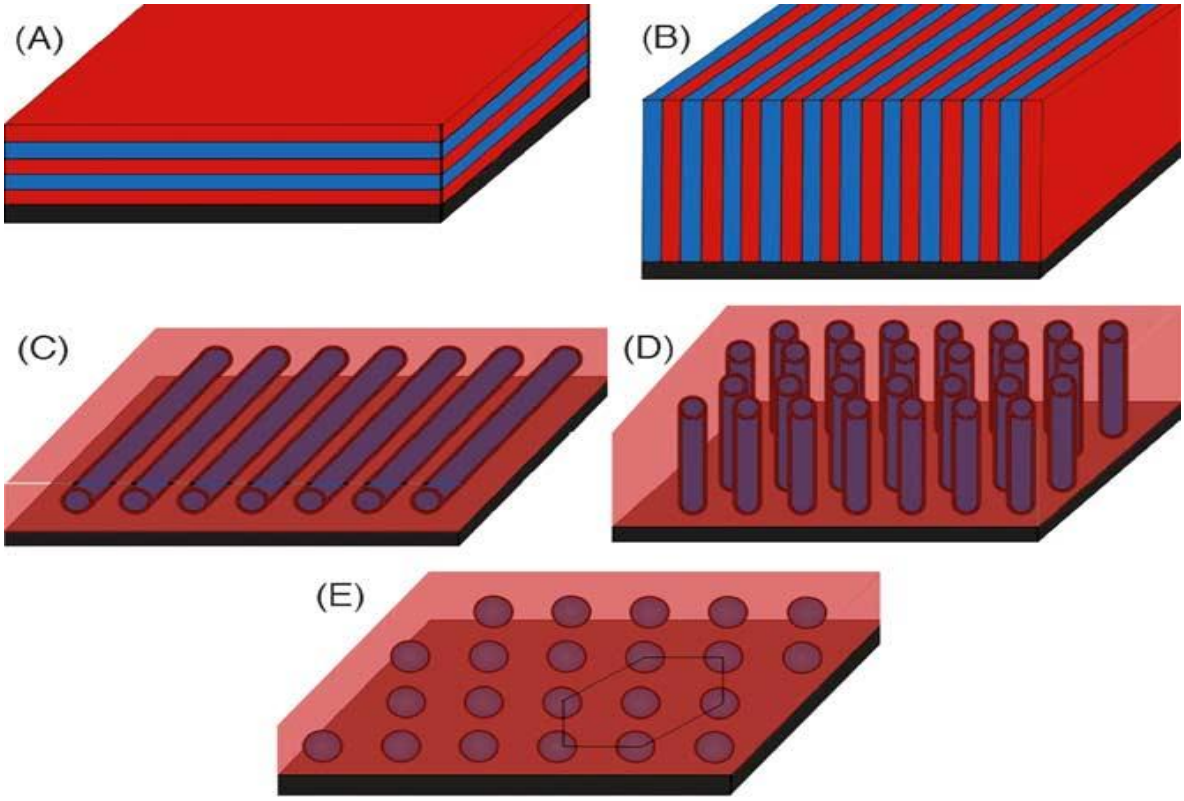

Fig 4. Orientation of BCP Domains with respect to surface of the substrates **(a)** & **(b)** Long axes cylinders and lamellae shape with the surface is a major characteristic of the BCP films. **(c)** & **(d)** Lamellae perpendicular to the surface and cylinder lying parallel, may have potential in the patterning of the Nanowires. (e) For the application of the data storages, upright cylinders and spheres can be of interest.

Patterning the substrate surfaces to control the random orientation of the BCP thin films for the application of fabrication of the micro and nano scale electronics and many biological application is quite important at nanometer scale. Although bulk applications for BCP films range from the drug delivery applications to nanometer structural materials.

These BCP self-assembled patterns have potential to be considered as nano-lithographic masks as well as templates for the further synthesis of nanometer scale structures. Self-assembly of BCP has provided a prospective route for the fabrication of small sized i.e. <50nm and dense pitch i.e. <100nm features with high and precise accuracy. However, the current requirement by the industry for practical applications, is a rapid, high-resolution method for patterning block-copolymers with different molecular weights and compositions across a wafer surfaces, with complex geometries and diverse feature sizes.

In order to make use of BCP thin films in nanoscale applications, it is only possible by exploiting contrasts in chemical or physical properties that lead to different etch rates or attractions to new BCPs materials. All of new applications, depend on the extremely regular self-assembly of block copolymers over macroscopic distances, i.e., optoelectronics, batteries, and fuel cells highly rely on the inherent properties of the blocks. However, the nano-domains and nano-patterns still need to be extremely controlled and oriented.

1.3.2 Lithographic Applications by BCP Self Assembly

BCPs have contributed significantly in fields of electronics, optoelectronics, magnetic storage devices, nanometer scale patterning, and in solid state LED lightening systems to fulfil the miniaturization demand. Because of their strong self-assembling properties, block copolymers are proved to be the potential candidate of next generation nanometer scale patterning techniques.

For lithographic techniques, nanolithography is very important to be achieved because of the ever increasing need of miniaturization. The minimμm size of the features that can be developed by conventional lithography strongly depends upon the wavelength of the immersion tool used for ultra violet light exposure machines. One of the techniques named as electron beam lithography, however, is still able to provide patterns of sizes ranging from 150nm to 30nm but it has limitations for its expensive cost and longer time duration that it takes to write features. While, using block copolymers, structures of ~150nm can be routinely produced, which awards block copolymers with an inevitable significance to overcome these limitations and to provide an improved alternative to conventional photo-lithography.

Besides nanolithography, block copolymers are widely used in development of organic and inorganic hybrid mesostructures. Single ceramic nano objects are being produced by thermal annealing treatment of these hybrid materials.

CHAPTER 2: LITERATURE REVIEW

2.1 Classical Lithographic Methods for Micro and Nano Electronics

A. Photo-Lithography

Photolithography, also known as UV lithography is a conventional method to transfer features or patterns on to the chemically treated substrates. It applies UV light to pass through the photomask (an image that has the desired features which are to be fabricated) and to shine on a photo sensitive material entitled as "photoresist" to make it either engraved into the substrate or popped up. Further the patterns are developed as similar to photography for etching the undesired photoresist.

Another technique, slightly different in concept, is called "Contact Photolithography" or "Contact Printing" which has all the similar principles. The only, difference is that in this type, there is no gap present between the photomask and the coated substrate. It has advantages when thick photoresist is to be patterned.

Although with photolithography process, features with nanometer scale can be obtained but due to its limitations it is quite difficult to continue with this process. Some of the major limitations are due to the wavelength, photoresist [11-12], and immersion optics [13-14] for the patterning which are listed as follows:

1) Resolution limit due to wavelength
2) Constraint of speed and time of patterning
3) Limit of immersion optical tools
4) Resolution limit due to photoresist
5) Cost of the overall process

The details of these issues would not be discussed here.

B. Projection Printing

This is another lithographic technique in which the photomask is placed nearer to the UV lamp instead to the substrate. The light is passed through opaque and transparent regions and then is passed from lenses to be focused on to the substrate sample. This technique was introduced to overcome the restrictions which were the main issues in contact photolithography. One of the first contribution was *phase shifting mask* [15-17], in which π phase change is present in between the projected light so that it may have zero intensity regions at destructive interference of the alternate black and white features.

C. Electron Beam Lithography

Electron Beam Lithography or E-beam Lithography is a method in which the patterns or shapes are written with a pen of focused and scanned beam of electrons on a surface coated with the electron sensitive material. This method was the first important feature of the Bell Labs [18]. Usually, a minimµm nµmber of picture elements that can be written with the e-beam pen is 25. If a chip has 1×10^{11} features which has say, 2.5×10^{12} picture elements, then the e-beam pen would take almost 8 hours to write chip patterns [19]. This is the major and important limitation of e-beam lithography. Despite the high quality of patterns achieved from e-beam, the difficulty of producing qualified desired photomasks by e-beam hindered serious development of fabricated patterns.

D. X-Ray Lithography

Another patterning method, called x-ray lithography, as the name suggests, uses x-rays as an exposure tool instead of UV light in photolithography. It is advantageous in terms of getting higher resolution as the wavelength of x-ray is much smaller than UV light. Different materials are used for x-rays lithography as it treats the matter quite differently. The x-ray lithography [20] provides with a wide range of wavelength from 0.4nm to 100nm due to which it is very suitable for nanolithography. Usually, materials with low atomic nµmber like diamonds, silicon, silicon carbide and polyimides are considered suitable for x-ray lithography. While in most of the cases, polymethyl methacrylate (PMMA) is a material of choice which works well.

X-ray lithography has advantages like, shorter wavelength, better speed than e-beam, simpler to use, high resolution and uniform refraction pattern. But again, this technique also suffers from quite a bit of limitations as, distortion in absorber, problems with focus and high costs issues for x-rays masks.

E. Patterning Techniques without Light Exposure

Unlike the fabrication processes discussed above which use light exposure to carve features in substrates, there are other patterning methods which do not actually use any sort of light exposure (i.e., electrons, photons or ions). The techniques use simple mechanical (i.e., templates) [21] or chemical (i.e., self-assembly) processes to shape material into desired structures.

Some well known techniques are described below:

(1) Nano-Imprint Lithography

Nano-Imprint lithography, as the name describes, shapes the material in to the desired structure of the pre-patterned molds. The mold, normally called as “master mold” can be used for repeated nµmber of times to form these structures [22].

NIL is very impressive and simple way to replicate patterns which can not only provide high throughput and can save time but is also highly cost effective. The major limitation though can be guessed as the deformation of the mold which would be used for nµmber of times to fabricate these patterns. The other types of the mechanical patterning techniques

are 1) thermal NIL, 2) Step and Flash NIL, 3) 3D Patterning 4) Injection molding 5) Micro-milling. The details would not be discussed here.

(2) Soft Lithography / Nano Printing

Another mechanical patterning technique called soft lithography or nano-printing is a process in which a polymer based ink is poured on to the pre patterned surface and then it is cured thermally to produce the negative replica of the desired patterns [23]. Soft lithography is mainly for the patterning sizes greater than 100 nm as the stiffness of the stamp and flow of the ink cannot be controlled in an efficient way.

(3) Self Assembly

Self-assembly is a chemical patterning technique, in which the material shapes itself into features. It has two types: 1) Unguided Self-assembly: in which the self-formed patterns are in micrometer ranges and are randomly oriented with no regularity. 2) Directed Self-assembly: also called templated self-assembly serves as a guide to educate self-assembly of the material by providing start to end information. With guided or directed self-assembly, sub 20nm channels can be produced routinely which is below the resolution of conventional lithography [24-27].

Currently, the research is still running in this self-assembly approaches to form structures and to come up with the solutions of the problems which are being faced such as density defects, edge roughness, materials chemical compatibility / surface treatments and for the accuracy of features.

2.2 International Technology Roadmap for Semiconductors

Scope

The International Technology Roadmap for Semiconductor (ITRS) are the sets of the docµments which are created by the group of semiconductor industry specilist and professionals. These docµments represents the many valuable and best point of view over a research into many innovative areas of technology, including time lines upto 15 years into the future. In the scope of ITRS roadmap, different lithographic techniques are discussed that are potentially available to cope the requirement of the current resolution and pattern quality to meet the future needs of the semiconductor industries. The previous chapter released have discussed the basic patterning requirements from 2014 to 2028 and for the first ITRS has include the contact hole pitches in a finFET fin half pitches. These fins are the smallest half pitches in a finFET containing chips which are introduced into production in 2012. The ITRS has also discussed the parameters i.e. wafer flatness requirement, chip size along with the nµmerical apertures (NA).

Difficult Challenges

In ITRS the challenges are classified as near term i.e. for 5 years approx, and long term challenges i.e. 2017 and beyond. In near term challenges the main focus are on multiple patterning and EUV. The major challenge for EUV is a driving source power. The over all cost and through put of EUV would be very uncomfortable with a proper enough source power. Direct self assembly can be one of a possibility, if it represent a enough low defects

and good patterns registration for short term simple patterns. ITRS sμmmary of the challenges are as follows:

Near Term Challenges (2013–2016)

Cost and cycle time of multiple patterning, Process controls i.e. overlay, CD control, LWR with multiple patterning, EUV Source power, EUV Mask Infrastructure, EUV resist, DSA defectivity and positional accuracy

Long Term Challenges (2017 and beyond)

Higher source power for EUV**,** Higher NA EUV tool, DSA compatible design rules, EUV Extension, Maskless lithography production tool demonstration, Imprint defectivity, throughput and OL matching.

Lithgraphy Technology Requirements

Lithography is one of the most practiced tool in semiconductors industry for the fabrication of the patterning different layers at several wavelenghts. Currently the highest resolution lithography is done by wavelength of 193 nm and immersion scanners with 1.35 NA lenses. For simple pattern production such as lines and spaces has a resolution limit of 40 nm half pitch with 193 nm wavelength.

Conventional lithography has been improved i.e. by increasing the nμmerical aperture (NA), decreasing the exposure wavelength and using improved advanced processes and materials. Because of lack of a lense material, a current lithography cannot achieve the optical wavelength of 157 nm. Therefore the industry has moved and develop a EUV

lithography with 13.5 nm wavelength with nµmerical aperture (NA) of 0.33 NA but there exist many challenges.

A further techniques are available for patterns multiplication which can be used for simple structures such that lines and spaces. For patterans multiplications, a multiple exposure process steps are performed which creates complicated tolerance stack ups and the process needs to be well controlled and optimized.

For high resolution patterns, E-bean lithography is used which writes and defines a patterns over a substrate in e-beam sensitive resist, which is slow and hence needs a massively parallel writings independently.

A nanoimprint lithography is a potential solution, in which a physically stamp is used in order to transfer a patterns from a high resolution mold to a liquid on a wafer. Since its physically contact method, a several defects occur and need to be handled with extra care.

The emerging techniques which has shown a great potential since last two years is a Directed Self Assembly (DSA). The patterns achieved from this techniques leverages the similar size of a polymer molecule. The most common used polymers are block copolymers which are controlled two different polymers made up of different monomers.

A detail chapter including challenges are available by ITRS on the topics discussed above briefly i.e. EUV lithography, Multiple Patterning / Spacer Technology, E-bean lithography, Nanoimprint lithography and DSA [28].

Emerging Research Materials Sμmmary

This chapter by ITRS includes to deal and address the new potential candidate materials for the reasearch challengaes in lithoraphy techniques. This chapter consist of the materials which would ultimately support the lithography, future memory and logic devices, front end processing, interconnects and assembly and packges.[29]

Difficult Challenges

The most difficult challenges of EMR are to have certain options on materials, multiple chemical and physical properties of materials, should have the potential to enable and enhance the high density of patterns, interconnects, operation at nano scale and packaging. Some of the challenges on materials are discussed below [30]:

Challenges (2013 - 2020)

- Attaining the desired physically and chemically properties in integraded patterns and structures.
- Smart and effective control over the defects in the fabrication and material processing.
- For DSA materials, highly controlled self assembly processes to come up with desired properties with high through put.
- Characterize and control coupled properties of embedded materails and their interface in lithography processes.
- Recognizing manufacturable methodologies to enable deterministic fabrication with required property control

Challenges (2021 - 2028)

- Accurate multiscale simulation for prediction of unit process the rsulting structure, properties and device performance.
- Metrology to characterize structure and properties of materials at the nanometers scale.
- Fundamental thermodynamic stability and fluctuation of materials and structures.
- Electric feild control of the electrochemical reaction in a nanoscale device and at an interface.
- Metrology to characterize defects at the nanometer scale with atomic resolution

2.3 Nano Lithography for Micro and Nano Electronics

The present improvements in photolithographic techniques have enabled the researchers to expect more than what was even believable in a past decade. The advantages of the techniques, either they are radiation based or non-radiation based patterning techniques, have capacitated the micro and nano-electronics to achieve exponential decrease in sizes for the IC features up-to the minimμm size called critical dimension.

The **Table 1.** Provides the significant comparisons of radiation based lithographic techniques in terms of their throughput and minimμm sizes of features that could be obtained.

Sr.	Radiation based Lithography Techniques	Minimμm Features Size	Throughput	Application Fields
1	Photo-Lithography (Contact and Proximity Printing)	2-3 μm [32]	High	MEMS devices, LOC devices
2	Photo-Lithography (Projection Printing)	Few tens of nanometers, 37nm [33]	Very high, ~80 wafers per hr [34]	Commercially produced IC and CPU chips [34]
4	Extended UV Lithography	<30 nm	High	Advanced IC and CPU chips
6	X-ray Lithography	10-20 nm	High	It can be used as complementary techniques but it is very expensive.
5	Ion beam Lithography	~20nm [33]	High	Patterning in R&D with hole arrays [35]
3	Electron beam Lithography	~ <5 nm[37]	Very low, 8 hrs to write one chip features [33-34]	Masks production [34], ICs and Nanofluidics patterns with hole arrays [36]
7	Scanning robe Lithography	Few tens of nanometers, [37-48]	Very low [37]	Bio-electronics, Bio-sensors and Biomedical devices [37,38,40]

Table 1. Specifications and Applications of Radiation based Lithographic Techniques [31]

While the **Table 2.** Provides the comparisons of non-radiation based patterning techniques in terms of their throughput and minimμm sizes of features and applications. These techniques create patterns by means of mechanical or chemical processes and hence do not use light exposure.

Sr.	Non-Radiation based Lithography Techniques	Minimμm Features Size	Throughput	Application Fields
1	Nano Imprint Lithography (NIL)	6-40 nm [41-43]	High, > 5 wafers per hr [34]	Bio Sensors, LOCs, Nano-channels [43-44]
2	Soft Lithography	few ten of nm to μm, 30nm [33, 45]	High	LOCs for microfluidics and various applications [45]
3	3D Printing	50-100 μm	High for small devices	Biomedical devices, micro/nano features making
4	Injection Molding	~ 500 nm – 5μm	very high	LOCs for various applications, nano-structures
5	Chemical Patterning / Self-Assembly	2-20 nm	High	Nano fabrications, Nano channels, Nanolithography

Table 2. Specifications and Applications of Non-Radiation based Lithographic Techniques [31]

2.4 Nano Lithography with BCPs

As discussed in the introduction to BCP thin films section, BCPs self-assembled patterns have a potential not only to provide nano-structures but also to be considered as nano-lithographic masks to aid the manufacture of nano-features for specially nano and microelectronics. This self-assembly attribute has provided a prospective track for the fabrication of the features <50nm with relatively high density and multiplexed geometries. Besides the current challenges which BCPs patterning is facing, these have many advantages over other patterning techniques which attracts the researchers to work in this field. There are some of the major benefits related to self-assembly of BCPs which are highlighted here [46]:

1) Control over length-scale

With self-assembled BCP thin films, micro-patterns with domains from 5-50 nm in length can be routinely produced with high and precise accuracy by just changing monomer-structures, temperature conditions and composition in synthesis of polymers.

2) Control over morphology

Diblock polymers demonstrate four various equilibriμm conformities: body-centered cubic arrays of spherical micelles, lamellae, gyroid and hexagonal cylinders. To regulate the morphological structure of BCPs into the desired shape, influencing factors like composition, temperature and diluents can be used in particular combinations [47].

3) Control over domain functionality

To select the each polymer for the desired purpose, the advancements of synthesis of block copolymers provide entire freedom to choose that particular polymer in a block of polymers. This is an interesting feature that provides each block to show properties of targeted applications.

4) Detention of traditional polymeric benefits

Like other polymers, block copolymers also possess the traditional advantages which include low cost, easy access, toughness, low density, flexibility and elastomeric properties.

Potential Advancements using BCP Nano-Lithography

The thermodynamic driving forces for block copolymers (BCPs) self-assembly are quite weak, thus leading the defects to be ensnared to the patterned surface. The concept of improved lithography and defect free directed block copolymer assembly was demonstrated in detail in year 2008 by Ricardo Ruiz et.at, [48], in which immaculate block copolymers arrays were directed at densities up to 1 terabit per square inch on chemically patterned surface of the substrates. Chemically treated substrates not only increased the densities of BCPs by a factor of four but also the size reduced by a factor of two while providing the improved dimensional uniformity at the same time. Multiplied and rectified block copolymer patterns which were achieved are shown in **Fig 5.**

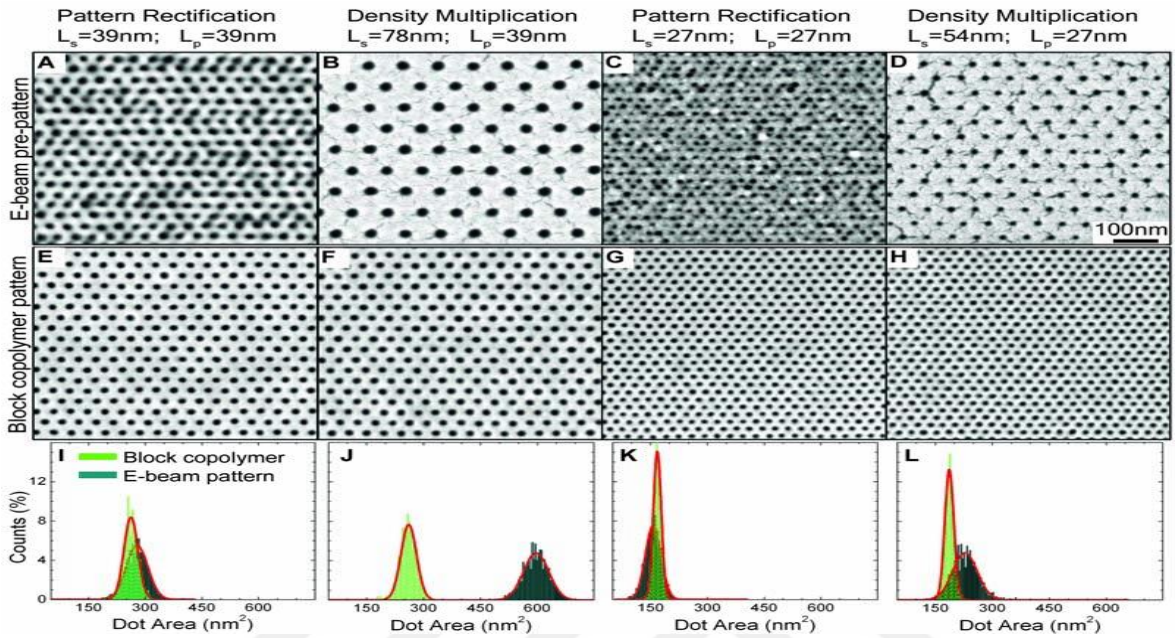

Fig 5. SEM images of Multiplied and Rectified Images [48]

One of the potential method for finding significant applications in nano fluidics and nano electronics, in year 2009, B. Radha and G.U. Kulkarni et.al [49], were successfully able to get Gold (Au) trenches of width ~30nm from the replica master of PDMS mold obtained from the CD patterns. In order to get around 30nm to 50nm grooves, the stamp and the substrate were heated (at 130˚C) above the glass transition temperature of the polymer, Tg (~94 ˚C). Glass like polymer started forming between the stamp relief structures which dewetted PDMS stamp internally and thus V-shaped grooves were formed due to interfacial forces. Furthermore, Au was deposited by physical vapor deposition technique on to the PS stamp to achieve ~30nm wide and ~18nm thick features as shown in **Fig 6**.

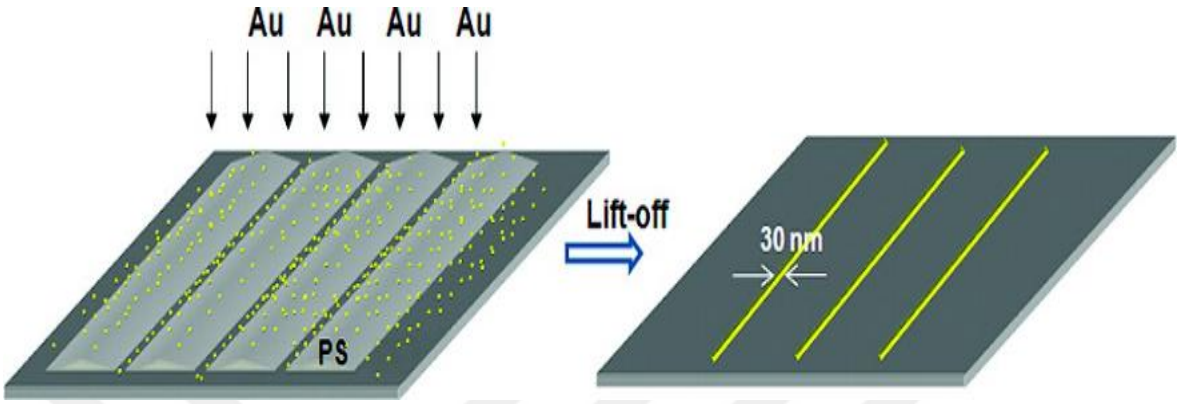

Fig 6. Metal Deposited Structures obtained from the PDMS stamp created from CD Structures [49]

An attempt to miniaturize block copolymer films of line widths sub-500nm was demonstrated by M. Serdar Onses et.al **[50]** in year 2013, in which ultrahigh resolution jet printing technique was used to pattern large areas with polystyrene BCPs of various weights and compositions. Printed geometries were having dimensions of sub-500nm (as shown in **Fig.7**) line widths and almost ~45nm line edge roughness. It was also reported that nano-domains of well-defined size and shape can be printed with repeatable periods by thermal annealing of simple, chemically treated or topographically featured substrates with ranges that could span from nanometer scale to centimeters. It was also suggested that with some modest adjustments, jet printing techniques can be used to other types of BCPs having diverse chemistry, morphology and self-assembling strategy.

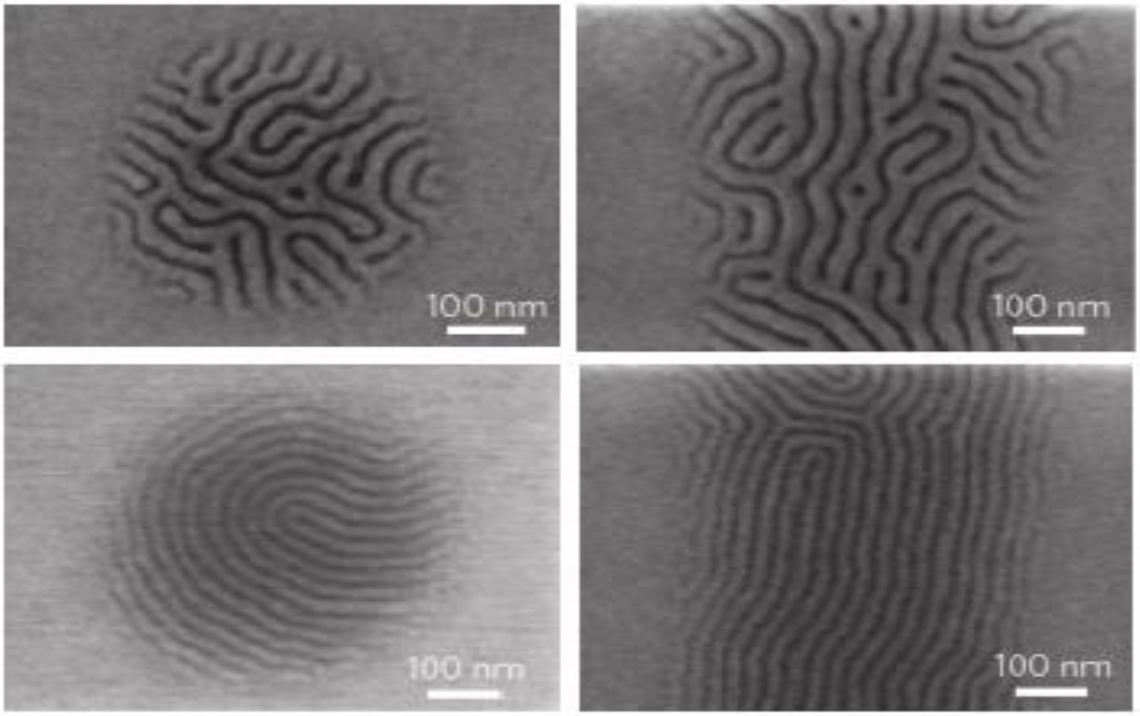

Fig 7. BCP deposited patterns using ultra high resolution ink-jet printer **[50]**

There are other great works also present in literature but those will not be discussed here.

CHAPTER 3: DESIGN METHODOLOGY

3.1 Overview of Large area Patterning of BCPs

A highly promising approach to fabrication of nano-patterns on large surfaces substrates is self-assembly of block-copolymers (BCPs). When confined in thin films, phase-separated BCPs can form patterns with dimensions and pitches as small as 5 nm and 10 nm, respectively. Additionally, self-assembly of BCPs can be guided with lithographic templates and highly aligned patterns can be obtained. As a result, 2013 edition of ITRS lists directed self-assembly of BCPs as one of the future lithography technology solutions. Beyond the electronics industry, BCPs have a broad application potential that includes fabrication of optical devices and membrane technology.

A particular challenge for the usage of BCP thin films in nanolithography applications is the constraints in the size, periodicity and geometry of the features that are to be patterned on large area surface. The most effective solution to this challenge is patterned deposition of BCP films via an electrohydrodynamic jet printer which has been reported in a study published in *Nature Nanotechnology* (2013) [50] by a group of researchers that include the principal investigator of the proposed project. This approach provides independent control of the size, periodicity and morphology of the self-assembled nanostructures.

The objective of this work is to develop a new method for fabrication of multiplex and hierarchical patterns with dimensions that span the scale of nanometers to centimeters, using patterned deposition of BCP films on large surfaces areas through a microfluidic (MF) molding method. This approach enables localized delivery of BCPs with different molecular weights and monomer fractions over large surface areas in short times (parallel processing) and thus provides independent control over the size, periodicity and morphology of the self-assembled nanostructures. This approach only uses elastomeric molds removing the need for customized setups. The repeated use of both the molds and lithographic templates that are employed to generate molds will lower the cost of the process. An additional capability will result from the in-situ mixing of different BCPs at predefined ratios enabling the size, periodicity and morphology of the self-assembled structures to be tuned with the MF system.

3.2 DESIGN METHODLOGY FLOW CHART

(1) Photo Lithography

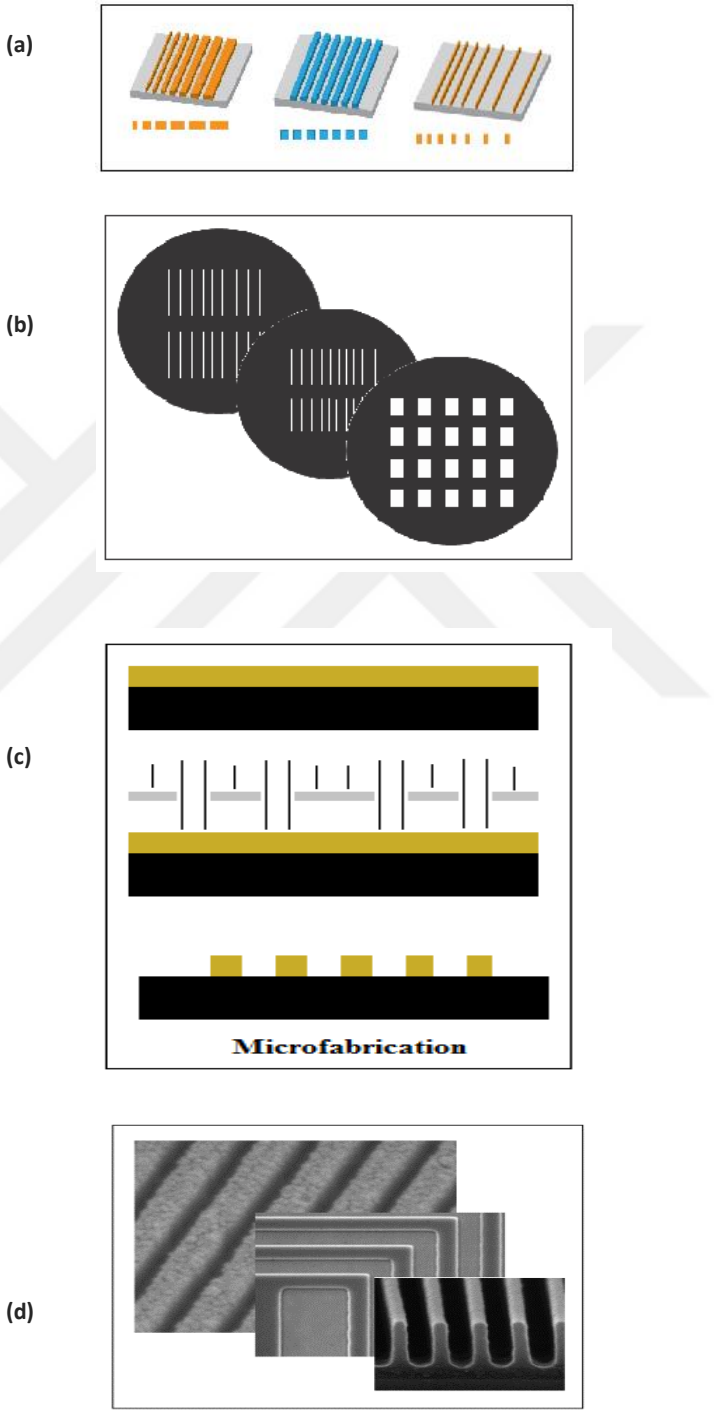

Fig. 8 (1): (a) Desired patterned structures for BCPs formation, **(b)** Different masks designs for achieving desired geometries, **(c)** Microfabrication Process of the designed structures for BCPs patterning, **(d)** Results for Microfabricated SU-8 Patterns

(2) Soft Lithography

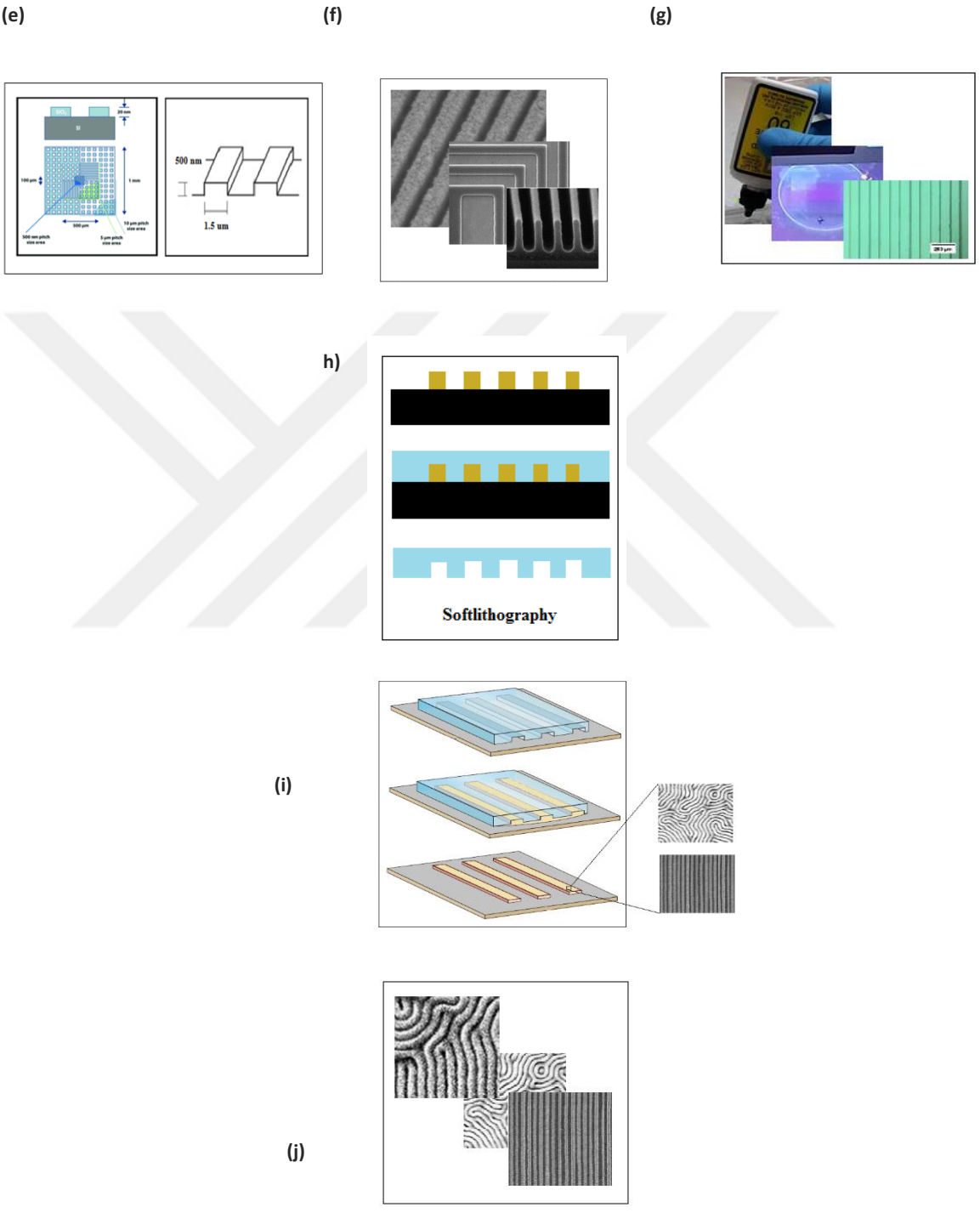

Fig. 8 (2): (e) Targeted AFM grids structures for Soft lithograpghy, **(f)** Fabricated SU-8 Patterns using Photolithography, **(g)**Targeted NOA Structures for BCP formation, **(h)** Soft Lithograpghy process to make PDMS Molds for all patterns achieved, **(i)** Formation of BCP patterns using PDMS molds, **(j)** Structures formed by Direct Self Assembly of BCPs

3.3 SU-8 Structure Design

3.3.1 Proposed Geometries

The ability of the micro-molding process using different targeted geometries have been investigated at this stage of the process specially to control the size, thickness and geometry of BCPs. In order to resolve the limitations for determining the size and geometry of the BCPs in the plane, dimensions and geometries are produced.

The parameters that changed basically in the micro-molding are being used as the mold of different width, height, frame ratio (aspect ratio or height / width ratio) of micro-channels and microchannel structure **Fig. 9.** First, the channel height is fixed **Fig. 9 (a),** the channel width is changed (and thus the frame ratio) to examine spontaneous regulations of BCP. In the next step, the channel width is fixed **Fig. 9 (b),** the heights of the channels are changed (and hence the frame ratio) in order to judge the effects on the thickness of the BCPs deposited. The thickness of the BCP films and the orientation of the nanostructures also play an important role in the transfer of patterns to the surface they are on. At this point, the BCP concentration of the solutions has also systematically varied to achieve access to different thickness ranges. Another version of geometry with varied interspaces between the channels is also targeted to check the resolution that a high resolution laser print could actually print on an acetate paper. This is elaborated in **Fig. 9 (c)**, and is used to gauge BCPs confinement into different width channels.

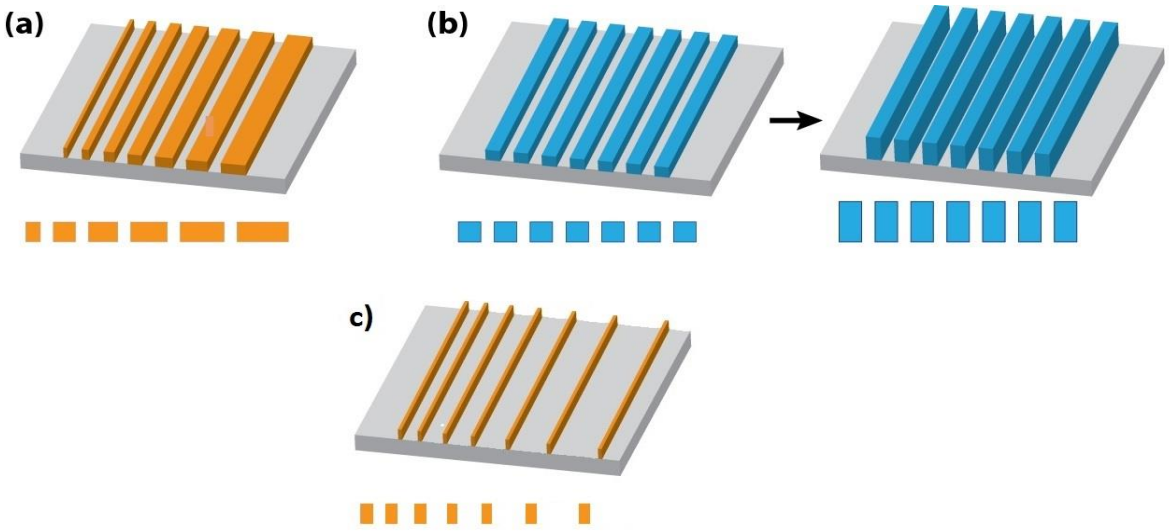

Fig 9. a) Width varying lines with same height, **b)** height varying lines with same width, **c)** Same width and height but varied interspaces in between lines

3.3.2 Lithography Photomask Design

Optimizing Dimensions for ultra-high resolution Laser Printer Acetate Mask

(a) 100u-10u width varying with 10u decrement

Initially, we have optimized the widths for the patterns in order to figure out the highest resolution of ultra-high resolution laser printers by using acetate masks by making different geometries of various dimensions. At the beginning we had designed the masks with the widths starting from 100 µm to 10 µm with 10 µm decrements. Masks were made using adobe illustrator software as shown in **Fig 10**.

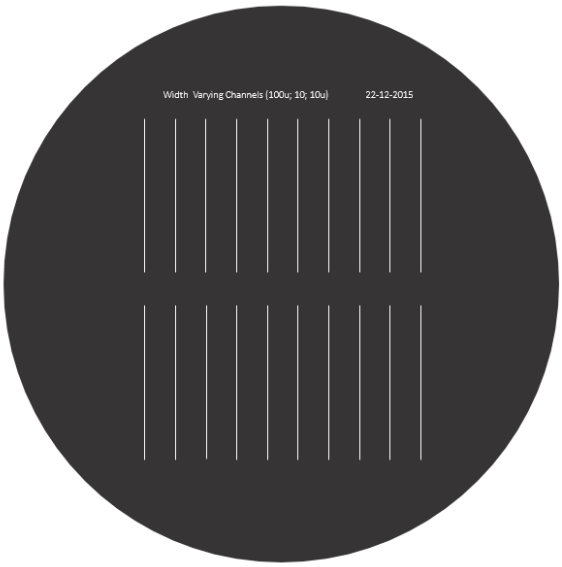

Fig 10. Width varying channels from 100 µm to 10 µm with 10 µm decrement

(b) 30 µm-2 µm width varying with 2 µm decrement

After the fabrication process for the above mask we noticed that the patterns below 30 µms were deteriorated. Therefore, we fabricated the features using new mask with widths ranging from 30 µm to 2 µm in order to know the lowest possible limit of the width which we could achieve through acetate mask. **Fig. 11** is the mask designed for the above mentioned ranges. The lithography recipe was kept almost same besides the UV exposure energy which was slightly higher this time.

(c) 20u width with 100u Inter-Space between Channels

The results of the mask discussed above clearly elaborated that the line widths below 20 µms were again deteriorating. Hence we concluded that acetate mask is not suitable to use below 20 µms for the widths of the features. Here, we created three different versions of

the mask having different heights i.e., 1µm, 5µm and 10µm but having same width sizes of 20µm. Interspaces between the features were optimized by testing and were fixed to be as 100µm to get the fine shapes of features. **Fig 12** shows this described design.

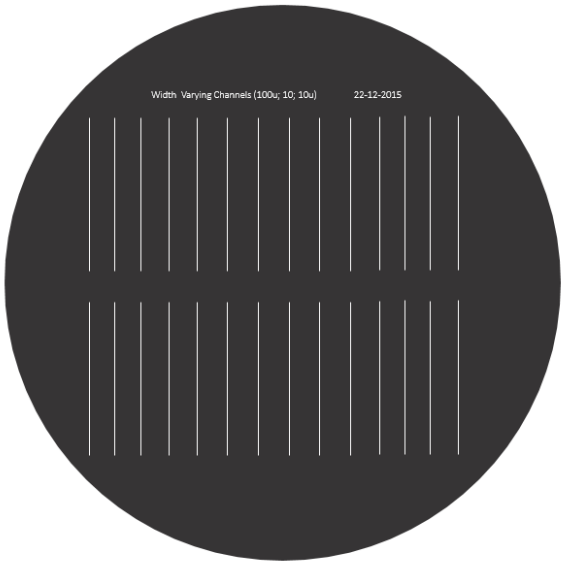

Fig 11. Width varying channels from 30 µm to 2 µm with 2 µm decrement

Fig 12. 100 lines in each set, Line width with 20 µm and Interspaces 100 µm

3.4 NOA Structure Design

Norland Optical Adhesive (NOA) is one of the auspicious UV-curable adhesive liquid photo polymer for low cost microfabrication structures. The main features NOA are as follows [51]:

- Low Shrinkage (1.5%) and Low Stress
- Strong Glass, Metal, Plastic Bonds
- UV Curing Intensity >2 mW/cm^2 @ 365 nm

NOA optical adhesive have an edge over the other optical adhesive systems because it eliminates the process of drying and premixing. The time which NOA takes in order to active the chemistry of photopolymer mainly depends upon the thickness, applied UV energy and distance from the source. In scope of our work, NOA based molds were fabricated in order to test the compatibility of the BCPs with NOA.

3.4.1 Geometry Design

For the compatibility of the BCP formation, a simple straight path channels are considered in order to flow the BCPs through them. This geometry has equal widths with equal interspaces between the channels.

3.4.2 Lithography Photomask Design

A chunk of small channels contain 100 lines with 20 µm widths and 100 µm interspaces each are designed on mask using Adobe Illustrator Software. Specially for getting the patterns on NOA, the negative of this mask was used. **Fig 13** shows the developed photomask for NOA structures.

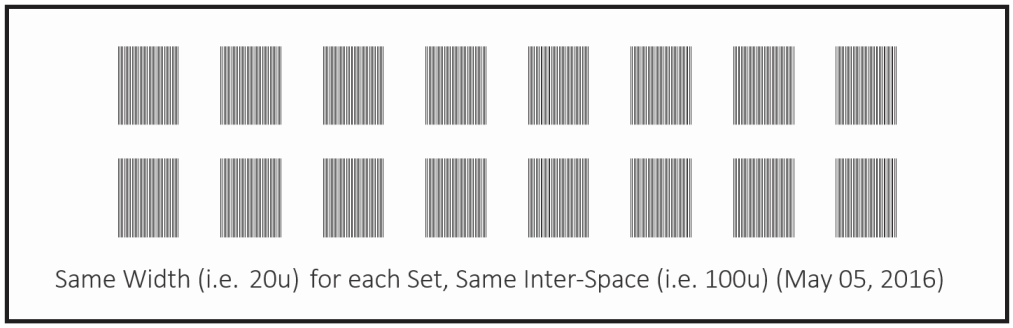

Fig 13: NOA mask with 20 µm line width and 100 µm interspaces

3.5 Atomic Force Microscopy Calibration Grid Structure Design

Atomic Force Microscopy (AFM) measures the features dimensions by translating mechanical probe over to the surface area. For this purpose, AFM uses some standard gratings with various models as reference. In this work, to get even narrower features in width specially, well aligned straight patterns with nanometer scale height are obtained using soft-lithography for two different models of AFM calibration grids having different dimensions. Their models type and schematics are described below.

3.5.1 Types of used AFM Grids

Two types of AFM grids that are used for getting the nanometer scale features are:

(a) TGZ3 Calibration Grid

Calibration grating TGZ3 is usually used for nonlinearity measurements and for one domain/axis calibration i.e., Z-axis. The structure step height for this grating is 520 ± 3 nm. . Basic step height can vary from the specified one within ±15 % depending on the batch (for example TGZ3 grating can have step height 580 ± 3 nm) [52].

(b) CS AFM Calibration Standard

The CS-20NG is a new grid standard of calibration grid that provides nanometer scaled level calibration using AFM apparatus. The XYZ calibration standard features silicon dioxide structures on a 5x5mm silicon chip are carved in order to provide complete three

dimensional XYZ calibration. Here, the calibration area is in the middle of the grating chip which can be easily seen by optical microscope as well. The step height for the structure is around 20nm. CS-20NG has three different x-y array sizes, all with the same 20nm height.

There are square pillars in the outer larger 1x1mm square and holes with a 10µm pitch. The middle square exhibits the lithographed circular pillars, holes and lines with a 5µm pitch. The small central area contains circular holes with a 500nm pitch. Vertical accuracy is 2% of the actual value which corresponds to ±0.4nm. The lateral pitch accuracy for the 5µm and 10µm patterns is 0.1µm. For the 500nm pitch region, the lateral accuracy is 10nm [53].

3.5.2 Structural Schematics and Specifications

Schematics of both of the gratings are given below. Also the general features sizes and specifications are also mentioned.

(a) TGZ3 Calibration Grid

General features of TGZ3 Calibration grid are given in **Table. 3.**

Sr.	Features Description	Features Specifications
1	Pattern Type	2-Dimensional
2	Structure	Si Bottom, SiO2 Step

3	Chip Size	5 x 5, 0.5 mm
4	Effective Area	Centered Square 3 x 3 mm
5	Period	3 ± 0.05 µm

Table. 3 Features description and specification of TGZ3 Calibration AFM Grating

Below is the schematic of TGZ3 calibration grating shown in **Fig. 14.**

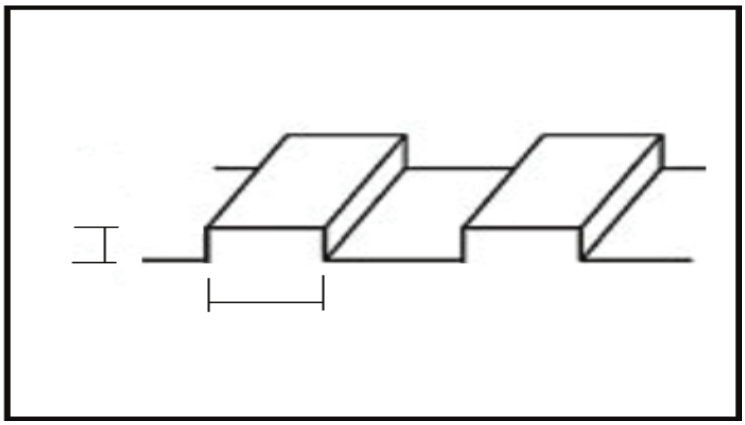

Fig 14. Schematic of TGZ3 calibration grating

(b) CS AFM Calibration Standard

General features of CS AFM Calibration grid are given in **Table. 4.**

Sr.	Features Description	Features Specifications
1	Pattern Type	3-Dimensional
2	Structure	Si Bottom, SiO2 Step
3	Chip Size	5 x 5 mm, 20 nm step height
4	Effective Area	Centered Square 500 x 500 µm

Table. 4 Features description and specification of CS AFM Calibration Grating

Below is the schematic of CS AFM calibration grating shown in **Fig. 15.**

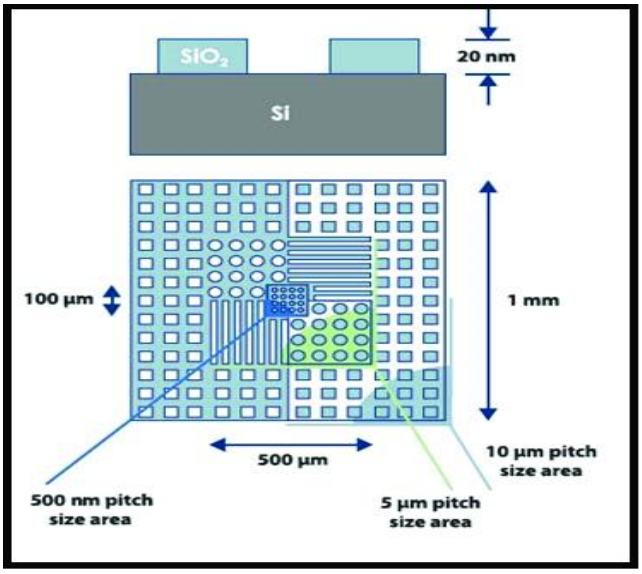

Fig 15. Schematic of CS AFM calibration grating

CHAPTER 4: FABRICATION AND EXPERIMENTAL SETUP

4.1 Microfabrication using SU-8

The advancements in photolithography literally brought the revolution in integrated circuits (IC) particularly from a decade by now. Almost all electronic devices that contain one or more ICs inside. Improving lithography techniques opened new avenues to produce smaller and smaller transistors, which further contributed in making faster and more efficient computing machines. Photolithography greatly empowered the progress of Micro Electro-Mechanical Systems (MEMS), which are more versatile in commercial products from mechanical to biomedical devices.

In general, the photolithography process consists of many detailed steps in order to fabricate desired device. Some of the main stages which are included in the overall process are spin casting, pre and post baking, light exposure to carve patterns and then developing. These steps and sub-processes may vary from different purposes and required devices.

PDMS and curing agent (Syllgard 184) were purchased from Dow Corning. SU-8 2050 was purchased from Microchem Inc. AFM calibration grid (629-30AFM) and Au NPs (20 nm

in diameter) were purchased from Ted Pella Inc. Silicon wafers < 100 > were purchased from Wafer World Inc. P2VP-OH (20.5 kg/mol) was purchased from Polymer Source Inc. Methanol, chloroform and *N*, *N* dimethylformamide, chlorobenzene were purchased from Merck. PEG (35.0 kg/mol, BioUltra), cyclopentanone, propylene glycol monomethyl ether acetate (PGMEA) and rhodamine 6G were purchased from Sigma-Aldrich.

SU-8 was diluted with cyclopentanone to achieve films of 10 µm in thickness by spin-coating at 3800 rpm. Patterns of SU-8 were then fabricated by photolithography: pre-bake (95 ^{o}C for 4 min.), UV exposure (~280 mJ/cm^{2}), post-bake (95 ^{o}C for 4 min.), development in PGMEA (5 min). AFM calibration grids were used directly without any processing. The elastomeric molds were prepared by casting the mixture (10:1) of the PDMS and curing agent on top of the master substrates followed by desiccation for 10 min and heating at 65 ^{o}C for 2 h. The cured PDMS molds were then separated from the master substrate. The detailed procedure of optimization from the photomasks to the fabrication protocols are discussed in further upcoming sections.

4.1.1 Optimization of Photomasks

Photomasks are generally images created on glass lithographic templates designed to optically transfer patterns on substrates such as silicon wafers, glass substrates or any other material in order to fabricate devices of all types. The pattern information transferred on a substrate is created in a drawing CAD tool and printed for lithography. Generally, Chrome coated glassy masks are used to transfer patterns optically on the substrate, but here Acetate

masks printed from a high resolution laser printer have been used for fabrication as they are easy to produce and are relatively less expensive. The optimization procedure for the producing the photomask is described as:

(a) Mask for an Individual Line and Chunk of lines

Initially a mask with single distant lines with greater interspace between each line and different width was designed in order to realize the throughput of the acetate mask. After optimization, a chunk of lines was designed with certain periods between various chunks. Each chunk was consisted of 100 lines.

(b) Optimization of Period between Bits of lines

After designing the set of chunks on 3-inch wafer, the interspaces/periods between each line in a group is optimized in order to understand the resolution of the dark regions using high resolution printer mask which could be able to fabricate the desired patterns using UV exposure. Here, one wafer was designed to have the total nμmber of 20 chunks.

(c) Dimensional (Length & Width) Optimization

After the initial test, widths for the patterns were optimized in order to figure out the highest resolution of the bright regions which could be printed using photo-lithography using masks obtained from ultra-high resolution laser. In the beginning, the masks with the widths starting from 100 μm and gradually decreasing upto 10 μm with 10 μm decrement were designed. It was observed, that patterns below 30 μm were being deteriorated and therefore a new mask with dimensions starting from 30 μm and decreasing upto 2 μm was

produced in order to know the lowest possible limit of the width that could have been printed by UV exposure tool.

The results of the mask discussed above clearly elaborated that the line widths below 20 µms were again deteriorating. ***Hence, it was concluded that acetate mask is not suitable to be used for fabrication of the features having width smaller than 20 µm.*** Similarly, the length of patterns was also selected to be smaller enough in order to make the capillary action of BCP successful. The optimized length was around half a centimetre which produced remarkable results.

(d) Height Adjustment: Here, three different versions of the photomask were created which had different heights i.e., 1 µm, 5 µm and 10 µm. The procedure of obtaining different desired heights included the dilution of the negative tone photoresist "SU-8" with cyclopentanon with certain concentrations which was also first tested and optimized.

(i) 1 µm Height: For obtaining 1µm height, SU-8 2050 was not only diluted highly by adding more cyclopentenon but also it was spun at highest rpm as 4500 rpm as mentioned below in **Table 5**. Also the UV exposure energy was decreased here to avoid over exposure and deterioration of patterns.

(ii) 5 µm Height: For obtaining 5µm height, the protocol which was used earlier to optimize was used here again with slightly less quantity of cyclopentanon added to SU-8 while having same UV exposure energy and spin coating rpm. Further details mentioned in the **Table 6**.

(ii) 10 µm Height: For obtaining 10µm height of the same mask, the new protocol had significantly lower concentration of cyclopentanon added to SU-8 2050 with lower spin rate i.e., 3500rpm and almost the same UV exposure energy. Further details mentioned in the **Table 7.**

Below are the tables which provide the complete protocols for the fabrication steps to achieve the desired heights of the features.

Sr.	Steps	Description of Procedures
1.	Photoresist Standard	SU-8 2050
2.	Dilution (if needed)	Diluted with Cyclopentenon to SU-8 Standard 2015
3.	Spin Rate	4500 RPM
4.	Pre-Bake	3-4 minutes at 95˚C
5.	UV Exposure	260-280 mJ/cm²
6.	Post Bake	3-4 minutes at 95˚C
7.	Developing	3-4 minutes in SU-8 Developer or PGMEA

Table. 5 Elaborates the entire recipe of lithography process for the patterns having thickness of 1 µm

Sr.	Steps	Description of Procedures
1.	Photoresist Standard	SU-8 2050
2.	Dilution (if needed)	Diluted with Cyclopentenon to SU-8 Standard 2015
3.	Spin Rate	3800 RPM

4.	Pre-Bake	3-4 minutes at 95˚C
5.	UV Exposure	300 mJ/cm²
6.	Post Bake	3-4 minutes at 95˚C
7.	Developing	3-4 minutes in SU-8 Developer or PGMEA

Table. 6 Elaborates the recipe protocol of lithography process for the patterns having thickness of 5 µm

Sr.	Steps	Description of Procedures
1.	Photoresist Standard	SU-8 2050
2.	Dilution (if needed)	Diluted with Cyclopentenon to SU-8 Standard 2015
3.	Spin Rate	3500 RPM
4.	Pre-Bake	3-4 minutes at 95˚C
5.	UV Exposure	300 mJ/cm²
6.	Post Bake	3-4 minutes at 95˚C
7.	Developing	3-4 minutes in SU-8 Developer or PGMEA

Table. 7 Elaborates the recipe protocol of lithography process for the patterns having thickness of 5 µm

(e) Finalized Photomask

Eventually, the photomasks containing all optimizations in one template were generated in which heights were optimized not only with the length and widths but also with the period

as explained above. The final mask contained same width sizes of 20µm, 0.5cm length and 100µm period between lines in a bit to get the fine shapes of required features.

This optimized mask was used for microfabrication using SU8 photoresist on 3-inch Si wafer as well as creating PDMS molds for the MIMIC process of BCP formation and PEG based structures.

4.1.2 Soft Lithography (PDMS) Templates

Soft lithography was done in order to get the PDMS molds/stamps out of the fabricated silicon wafer with different heights i.e., 1µm, 5µm and 10µm.

First, silicon wafers were salinized for 10 minutes with 3-Aminopropyl triethoxysilane. The PDMS was made by adding PDMS agent to the PDMS base in 1:10 ratio. After the PDMS desiccation process, the PDMS solution was poured over the salinized silicon wafers and was cured in an oven at certain temperature. When the PDMS was cured, it was cut out and separated from the wafer for further patterning process. Quantitative details for the soft lithography procedure are mentioned in **Table 8** below:

Sr.	Steps	Quantitative Description
1.	PDMS Base	25 gram in quantity
2.	PDMS Agent	2.5 gram in quantity (1:10 ratio of agent to base)
3.	Silane APTES quantity	50 µL

4.	Desiccation of PDMS	~15 minutes
5.	Curing PDMS	~2 hours at 65 ˚C

Table. 8 Explains the Soft Lithography Protocol recipe for creating PDMS elastomeric molds

4.2 Microfabrication using NOA

NOA based molds were fabricated in order to test the compatibility of the BCPs and PEGs with NOA. Initially, PDMS molds of different heights were fabricated by using photo and soft lithography, and then NOA was spun on a glass cover slip. A PDMS mold fabricated earlier was gently placed over the NOA coated glass cover slip and then was cured by UV lamp for an optimized time. Finally after curing, the PDMS molds were removed to obtain features on NOA stamps and were cured in an oven for almost 12 hours. The overall NOA molds process includes first the microfabrication, then soft-lithography process to obtain PDMS stamps and finally NOA features fabrication steps as detailed below along with their respective protocol in **Table 9.**

First, required features were fabricated on glass cover slip using "**20u width with 100u Inter-Space between Channels"** mask as explained in "section 3.3.2" to achieve height around 5µm for features.

Sr.	Steps	Description of Procedures
Sr.	Steps	Quantitative Description
2.	Dilution (if needed)	Diluted with Cyclopentenon to SU-8 Standard 2015
3.	Spin Rate	3800 RPM
4.	Pre-Bake	3-4 minutes at 95˚C
5.	UV Exposure	300 mJ/cm²
6.	Post Bake	3-4 minutes at 95˚C
7.	Developing	3-4 minutes in SU-8 Developer or PGMEA

Table. 9 Explains the photolithography procedure steps for making a template to be used for Soft Lithography which further would contribute to provide features on NOA coated glass

4.2.1 Soft-lithographic (PDMS) Templates:

Soft lithography procedure is same for every stage. The universal protocol of 1:10 of PDMS agent to PDMS base is used and finally PDMS stamps were taken out with details mentioned in a **Table. 10** as below:

1.	PDMS Base	25 gram in quantity
2.	PDMS Agent	2.5 gram in quantity (1:10) ratio
3.	Silane APTES quantity	50uL
4.	Desiccation of PDMS	~15 minutes
5.	Curing PDMS	~2 hours at 65 ˚C

Table. 10 Explains the Soft Lithography Protocol recipe for creating PDMS elastomeric molds

4.2.2 Fabrication of NOA Structures using PDMS Templates:

To finally get features on NOA coated substrates, the protocol used is described below in a **Table. 11** as follows:

Sr.	Steps	Procedural Description
1.	NOA Spinning	Spin NOA on cover slips on 2200RPM
2.	PDMS Stamp Embossing	Emboss PDMS stamp on coated NOA coverslips
3.	UV Exposure	Expose to UV for 3 minutes
4.	PDMS Stamp Removal	Peel off PDMS stamp gently
5.	Curing NOA Patterns	For ~12 hours at 65 ˚C

Table. 11 Explains the NOA patterning procedure through PDMS elastomeric molds

4.3 Microfabrication using Atomic Force Microscopy Calibration Grids

Atomic-force microscopy (AFM) is a very-high-resolution type of scanning probe microscopy (SPM), which can measure the surface patterns or roughness till the resolution on the order of fractions of a nanometer. For this purpose, AFM uses some standard gratings with various models as reference. To get even narrower features in width specially, well aligned straight patterns with nano meter scale height were obtained using soft-lithography for two different models of AFM calibration grids having different dimensions.

While in optimization process of both mask and features through microfabrication, maximµm feature limit of the mask and its throughput in term of feature size were observed. Desirable patterns dimension below 20µm width were not achievable. It was observed that on high spin rate such that below 1µm height, the channel walls of 20µm width were getting rough and deteriorating, hence another technique was required to get below 20 µm in width and below 1µm height in order to make the capillary action of BCP successful in PDMS channels.

In this work, to get narrower features in width specially, well aligned straight patterns with nanometer scale height are obtained using soft-lithography for two different models of AFM calibration grids having different dimensions. Their models types are described below:

(i) TGZ3 Calibration Grid

(ii) CS AFM Calibration Standard

The detailed dimensions regarding the AFM calibration grids which are used to create a PDMS molds for BCP formations are described in section 3.5.

4.3.1 Protocols for Soft-lithographic (PDMS) Templates

First, AFM calibration grids were salinized for 20 minutes with 3-Aminopropyl triethoxysilane. The PDMS was made by adding PDMS agent to the PDMS base in 1:10 ratio. After the PDMS desiccation process, the PDMS solution was poured over the salinized grids and was cured in an oven at certain temperature. When the PDMS was cured, it was cut out and separated from the AF for further patterning process. Quantitative details for the soft lithography procedure are mentioned in **Table 12** below:

Sr.	Steps	Quantitative Description
1.	PDMS Base	15 gram in quantity
2.	PDMS Agent	1.5 gram in quantity (1:10) ratio
3.	Silane APTES quantity	50uL

4.	Desiccation of PDMS	~15 minutes
5.	Curing PDMS	~3 hours at 65 ˚C

Table. 12 Explains the soft lithography procedure to make PDMS molds of AFM grids structures

4.3.2 Examples for Obtained Structures

These are the grids which are targeted to achieve patterns of bits and lines and dot structures **Fig 16, 17,18**. The dimensional and structural details are given section 3.5 in chapter 3.

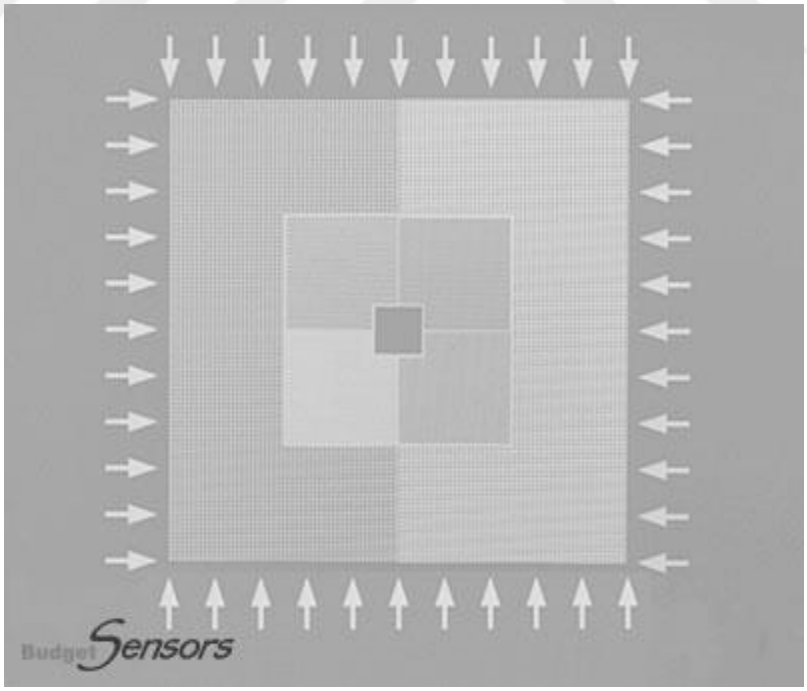

Fig 16: Examples of CS AFM Callibration Grid features containing bits and lines.

(a) Examples of features for AFM Grid with bits and lines

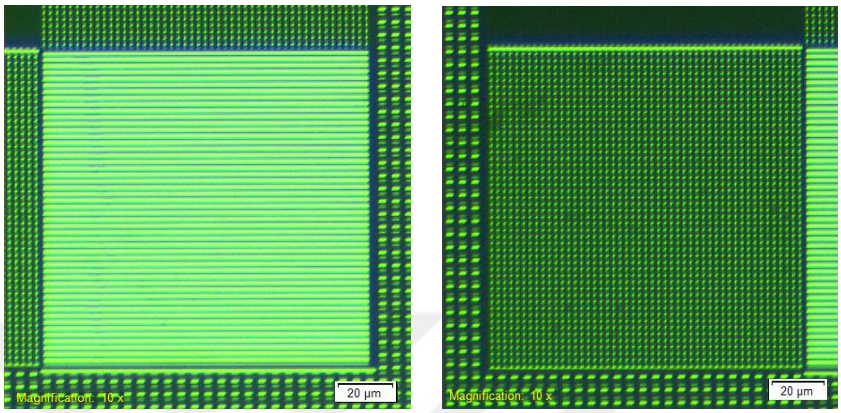

Fig 17: Fabricated PDMS molds of the AFM calibration grid with 500 µm x 500 µm chip size area

(b) Examples of features for AFM Grid with straight lines

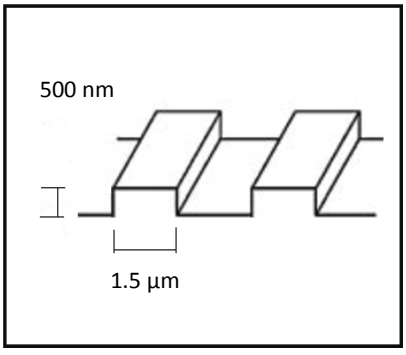

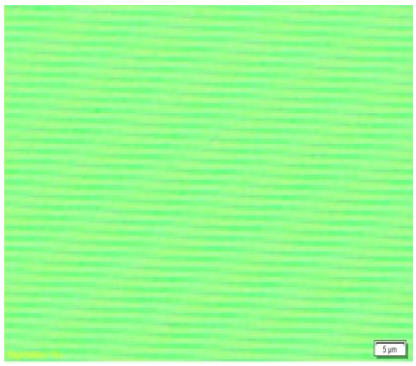

Fig 18: Fabricated PDMS molds of the AFM calibration grid with 5 x 5 x 0.5mm chip size area

CHAPTER 5: PATTERNING POLYMER BRUSHES AND BCP FILMS

5.1 MIMIC Background and Significance

Micro molding in Capillaries is an easy process which is highly being used in micro and nanofluidics because of its simplicity and immense significance. This procedural concept was first presented in year 1996, by George M. Whitesides et.al **[54]** and was referred and entitled as MIMIC. This procedure was based on spontaneous capillary flow action for filling nano and micro channels by a fluid. One of the major strength of this process is the surface chemistry of the substrate which plays a crucial role for filling the capillaries.

The significance of this procedure is that complex polymeric structures can be produced with single step using elastomeric molds of the stamps of the desired features. This one of the major process which not only supports the fabrication of nano and micro-structures but it also broadened the avenues of sub-nano features which could not be attained from conventional fabrication techniques. Another major importance of micro molding in capillary action is that this overall procedure is very simple to perform. Ease of fabrication is the key point which made MIMIC influential fabrication technique to employ and to produce patterns below ~20nm.

5.2 MIMIC Mechanism Description

A simple method was reported by George M. Whitesides et.al **[54]** to get patterns of required material by first placing the PDMS elastomeric stamps on the substrates and to fill the channels with required fluid containing the material to be patterned. After annealing on specific temperatures, solutes of the required material gets deposited on substrates while solvent evaporates. Schematic of the MIMIC procedure is shown in **Fig 19.**

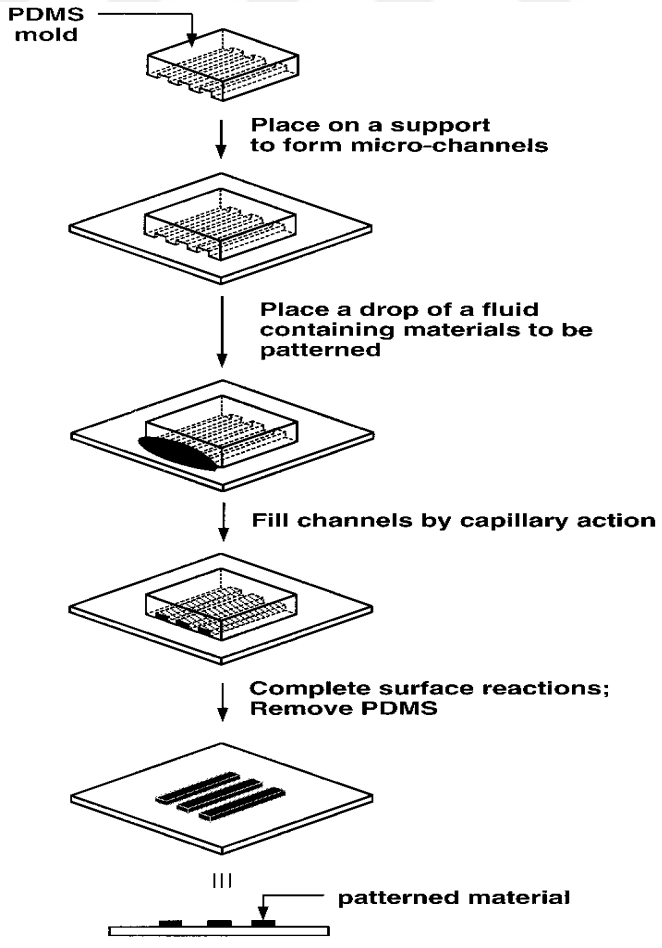

Fig 19. Micromolding in Capillaries Process flow **[54]**

5.2.1 Capillary Flow Action

Capillary flow action is one of the strength of microfluidic systems through which various advancements have been achieved in microfluidics field especially in lab on chip LoC devices. Capillary flow effects takes place particularly on the edges or the interfaces of the two mediμms such as liquid and gas or air. At interfaces, the surface tension according to the area of the interface exerts a force to pull the liquid droplets into the capillary. The details of this phenomena would not be discussed here.

5.2.2 Pre-Pattering Chemical Treatment of Substrate and Molds

Before patterning the substrates with BCP films or PEG polymer brushes, both the substrate and the microfluidic elastomeric PDMS molds of desired features, produced earlier were treated chemically to enhance the adhesion of the PDMS mold over the substrate. Pre-patterning chemical treatment is not only necessary for the adhesion purposes of the PDMS stamp over the substrate but also for avoiding any contamination and swelling problems of PDMS which are easily expected while dealing with it. Therefore, two types of chemicals were used for this reason which are discussed in detail in upcoming sections one of which was proved to be suitable for PDMS templates.

5.3 Patterning Polymer Brushes

5.3.1 Patterning of P2VP and PEG brushes using MIMIC

The PDMS molds were washed in DMF under sonication for 10 min and then dried at 90 ^{o}C for 2 hours, prior to the MIMIC process. PDMS molds were then placed on top of the silicon substrates that were freshly cleaned in a UV-ozone chamber (Bioforce, procleaner) for 20 minutes. Solutions (~5 uL) of (1% for AFM grids, 3% for 20 µm wide channels) P2VP-OH in DMF and (1% for AFM grids, 6% for 20 µm wide channels) PEG in methanol were placed near the open-end of the micro-channels. The molds were then removed from the silicon substrate following the filling of the channels and evaporation of the solvents which were monitored under an optical microscope. This process typically took ~2 h. The silicon substrates with the patterns of end-functional polymers were then annealed in a glove-box filled with argon at 180 ^{o}C for 5 min for the grafting of chains. The excess and ungrafted polymers were then removed by 3 cycles of sonication in solvents (DMF for P2VP and chloroform for PEG) for 3 min per cycle. The substrates were then dried with nitrogen.

5.3.2. Selective Immobilization of Plasmonic Nanoparticles on the Patterned Surfaces

Substrates containing patterned substrates were treated with citrate-stabilized Au Nano-particles (NPs) by spotting a droplet (~100 µL) of particle solution for 1 hour in a hµmid atmosphere. The substrate was then washed in water under sonication for 2 minutes and dried with nitrogen. A solution of 100 µm rhodamine 6G in ethanol was dropped on the immobilized NPs for investigating the SERS response of the particles **Fig. 20**.

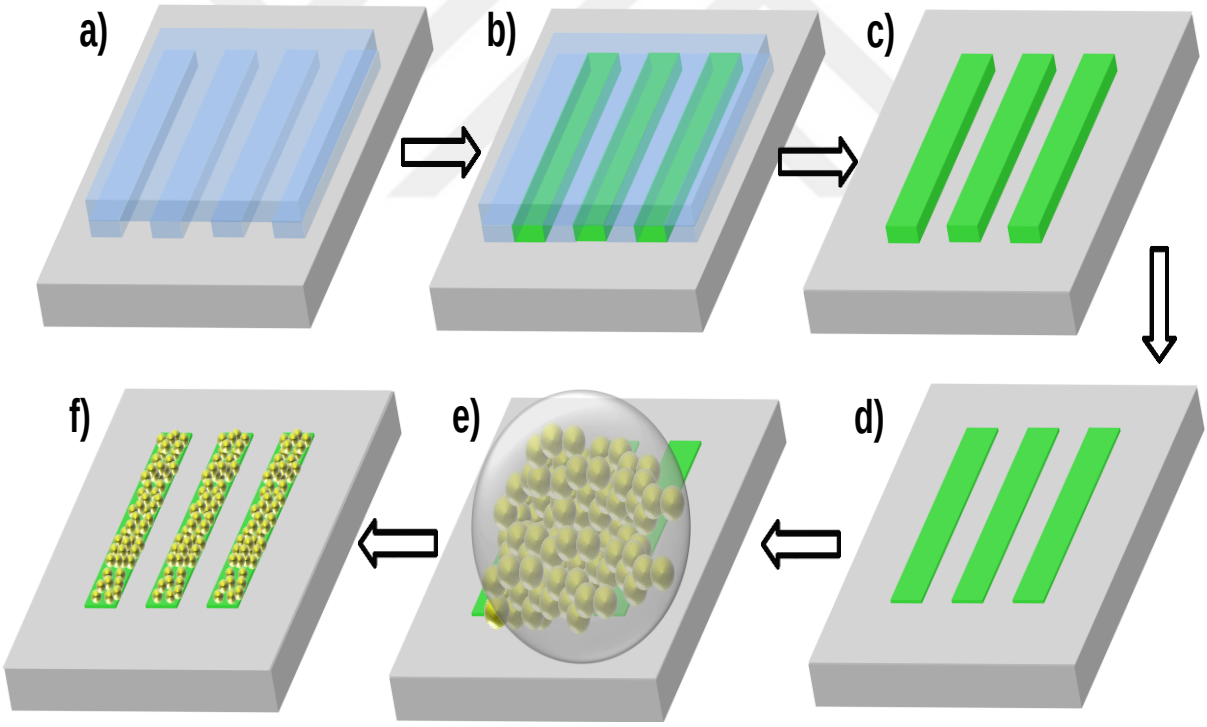

Fig 20. Schematic description of the process for fabricating arrays of plasmonic NPs on top of patterns of polymer brushes prepared by a soft-lithography approach. a) An elastomeric mold consisting of PDMS is placed on a silicon substrate forming open-ended channels. b) A drop of end-functional polymers dissolved in an organic solvent is placed at the end of the channels. The polymer solution fills the channel by capillary action. Two polymers are used: hydroxyl-terminated P2VP dissolved in DMF and PEG dissolved in methanol. c) Separation of the mold leads to patterns of end-functional polymers. d) A thermal annealing followed by washing of the excess material leads to grafted polymer chains on the areas defined by the channels. e) A drop of colloidal Au NPs is placed on the entire substrate. f) Au NPs specifically bind to the patterns of polymer brushes.

5.4 Patterning of BCP Films

5.4.1 Production of Microfluidic Molds

In the first step of the process, BCPs (block-copolymers) are targeted to be deposited locally on the surface by an approach known as micromolding in capillaries. In this direction, first elastomeric molds with microfluidic (MA) ducts were produced. For this purpose, SU-8 was first deposited on a silicon plate by spin-coating. Masks with patterns designed in computer-aided drawing programs are provided as ready.

These masks typically consist of chrome sections that pass through the light and block the passage of light. In regions where light passes **Fig. 21 (a)**, the photoresist is cross-linked and becomes insoluble in organic solvents. By taking advantage of this resolution, the photoresist in the areas not in contact with light was removed from the mediμm. Thus, the patterns shown in **Fig. 21 (b)** are obtained.

A polydimethylsiloxane (PDMS) prepolymer mixture, which is an elastomeric material, is cast onto these patterns **Fig. 21 (c)**. The PDMS precursor blend consists of two components, monomer and curing, which are generally mixed in a ratio of 10: 1. PDMS with different hardness can be obtained by changing the mixing ratio. The PDMS precursor mixture is cured for 1-2 hours at 65 ° C after being placed on the molds. After this treatment, the cured PDMS is elastomeric, **Fig. 21 (d).** Molds were prepared by separating the PDMS from the surface.

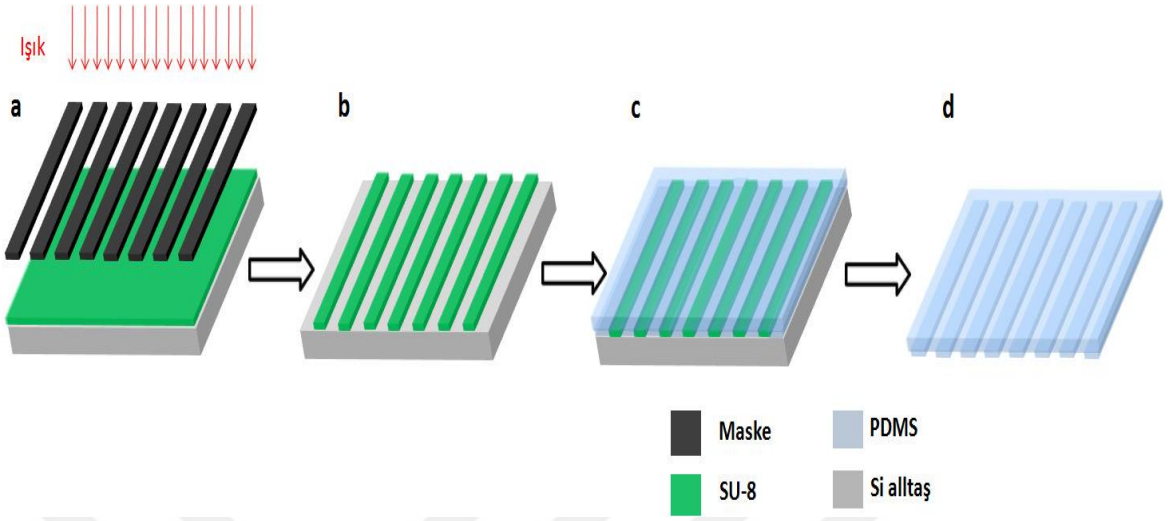

Fig. 21. Production of micro-molds. a) Photoresist patterning by light, b) Removal of photoresist that is not exposed to light, c) Pouring of the PDMS precursor polymer onto the photoresist template, d) Curing of PDMS and subsequent separation from the surface.

5.4.2 Selective Accμmulation of BCPs on Surface using Microfluidic Molds

This work of the project was aimed to deposit block copolymers (BCPs) on the surface with microfluidic (MA) molds. In this approach schematically illustrated in **Fig. 22** and **23**, the molds comprising three open microchannel structures are produced with the help of templates produced by lithography from elastomeric polydimethylsiloxane (PDMS) material. By placing these plates on the substrate, three open microfluidic channels are obtained. In other words, the open sides of the channels are covered by the sub-surface. Patterning is carried out by providing a solution containing poly (styrene-block-methyl methacrylate) (PS-b-PMMA) from the openings at the ends of these molds and drawing the

solution into the microtubes of the effector microspheres. Over time, in the evaporation of the solvent, only the BCPs remain in the channels and thus the BCP films deposited on the surface as a result of being separated from the surface of the mold are obtained. With the heating of the substrate surface containing these films, the BCPs undergo phase decomposition and nano-sized structures are formed spontaneously.

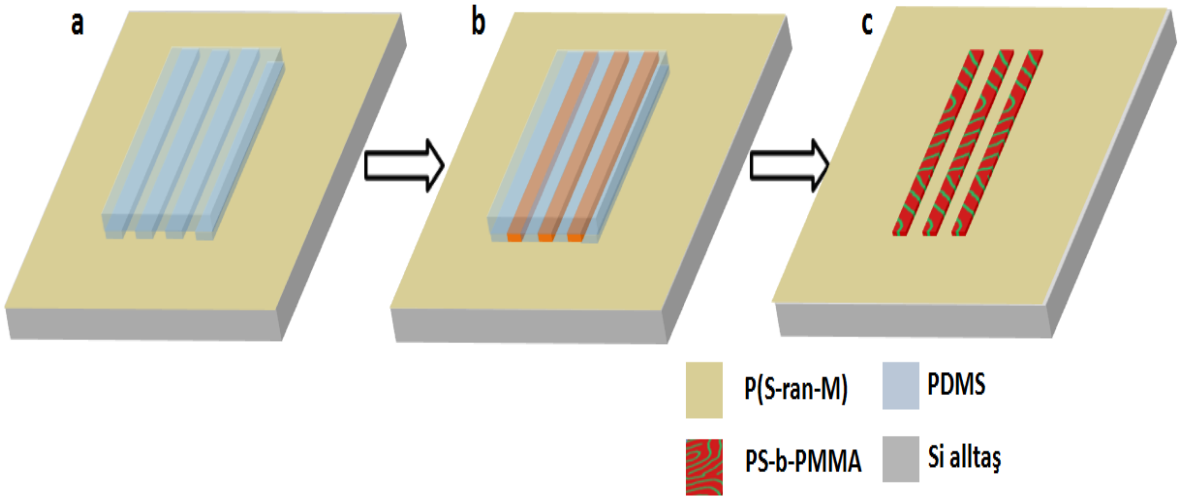

Fig 22. Schematic representation of BCPs patterning by micro-molding. a) Micro-molds are placed on the surface. The surface was functionalized with P (S-ran-M) with a randomly distributed copolymer containing styrene and methyl methacrylate so that the PS-b-PMMA had an upright orientation. b) In the second stage, BCP-containing solution containers from the open ends of the channels are effectively introduced into the channels. c) At last stage the mold is separated from the surface and patterns are formed by heat treatment and self-regulation of BCPs.

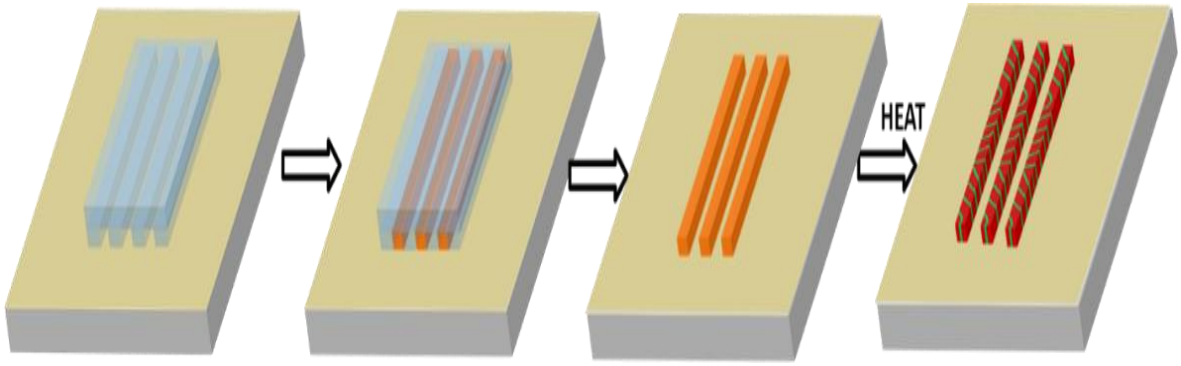

Fig 23. Filling BCPs with microfluidic channels

5.4.3 BCPs and its Solvent Selection

The solvent to be used in filling the molds with BCPs has critical prescription. The reason is that this solution determines the interactions of the BCP solution with both the substrate surface and the molds. Since the BCP solution is expected to fill the channels with the effect before applying an external pressure, the surface tension of the solvent and the wetting angle of both the allotter and the channel surface are important. Accordingly, it is expected that solvents with low surface tension and low contact angle with channel surfaces will be more successful. The solvent used from the other side should be able to solve BCP easily and have no effect on the spontaneous regeneration process.

In the classical works made by spin coating with PS-b-PMMA, toluene is used as a solvent. In this direction, firstly experiments with toluene were carried out. However, the toluene swells the PDMS molds and removes the conformal contact between the substrate and the mold, causing the solution to spread over the entire surface.

It was then decided to work with a small amount of solvent that swells PDMS with dimethylformamide (DMF), which can dissolve PS-b-PMMA and work with other BCP. As a result of using the DMF as a solvent, the problem of solubility of PDMS with conformal contact with matrix has been solved.

Before deciding to work with DMF, work has been done on spin coating of PS-b-PMMA with this solvent. Accordingly, 66000-63500 g / mol of PS-b-PMMA in a 1% DMF

solution was surface-coated on the random copolymer-functionalized surface. It was observed that after heating the BCP structure does not form uniformly along the surface. For this reason, the experiment was repeated by increasing the polymer concentration to 3%. The concentration of the polymer was increased and the formation of the structure was investigated. At this concentration, it was observed that the structure was uniform. For this reason, it has been decided to work with DMF in experiments.

5.4.4 BCPs Annealing Mechanism and Conditions

The accµmulation of BCPs on the surface with microfluidic channels has generally been carried out as follows. The molds prepared as described above were first rinsed under ultrasound in DMF for 10 minutes. After drying with nitrogen gas, the molds were dried for 2 hours on a heating plate at 90 ° C. The molds were placed on silicon substrate functioned with P (S-ran-M). In order to ensure conformal contact of the PDMS with the silicon ink, a slight pressure was applied from the top.

The pressure was removed after the contact was made. Then about 20 uL of solution was placed around the open end of the channels. The mold was separated from the surface after the solvent has filled the channels and then has evaporated. Substrate containing patterned BCP films was then heated in a glove box environment at 220 ° C or 250 ° C for 5 minutes.

5.4.5 BCP Self Assembly

Two factors necessary for the healthy running of this research were the preparation of a random copolymer-functionalized substrate surface and the display of self-assembled nanostructures. Here, the films produced by spin coating of BCP films were studied.

The orientation of the blocks must be perpendicular to the substrate surface so that the structures that the BCPs form can be used in designing different materials. Thus, when one of the blocks is removed from the environment, resist-like structures resulting from lithography and patterning were obtained. For this purpose, after the silicon substrate has been cleaned freshly with UV-ozone, it was functionalized with a polymer, P (S-ran-M), with a random distribution of styrene and methyl metacrylate. During the phase decomposition of the block copolymer, the random copolymer presents a uniform surface energy on both blocks, thus preventing any of the blocks from preferring the surface **Fig. 24**.

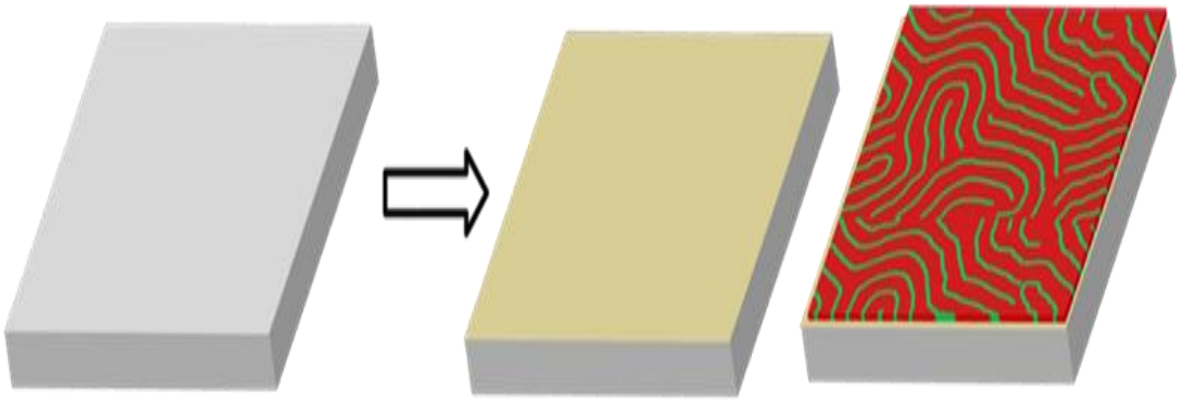

Fig 24. Phase separation of the blocks in a perpendicular orientation to the surface on the P (S-ran-M) functionalized substrate with the randomly distributed copolymer

In this direction, P (S-ran-M) with 57% styrene was deposited on the surface by spin coating with 0.25% of toluene solution. The film thickness measured by an ellipsometer is ~ 8 nm. This film is then placed in a glove box environment at 250 ° C for 5 minutes. It has been heated up. During this heating, cross-linking with glycidyl methacrylate in the copolymer was achieved. After washing three times under sonication with toluene, the crosslinked mat made up of styrene and methyl methacrylate became ready. BCP films were deposited on this surface by spin coating or MA molds. BCP films were heated in a glove box for 5 minutes at 250 ° C to allow for phase separation. More details on depositing with MA dies are given in results, in this section we have worked with films deposited with spin coating to test the success of sub-cast modification and the display of BCPs. Accµmulation of BCPs to the surface by spin coating was carried out with 1% of toluene solution.

5.4.5.1 BCP Directed Self Assembly

20 µms wide channels formed by photolithography revealed that the BCP nanowires were formed in large quantities, Figures are given in results section in chapter 6. In this BCP composition, further studies have been carried out on the control of solvent evaporation during the test. Experiments in a closed environment for the slowing of the evaporation rate have shown that BCP constructions do not occur. It has been seen that the nanostructures can be formed homogeneously in studies made with channels with a width of 1.5 µms, which were achieved by using AFM calibration grids. It has been found that BCP structures are seen homogeneously in the entire linear patterns arranged one after the other. More details are discussed in the results chapter 6.

CHAPTER 6: RESULTS AND DISCUSSIONS

This chapter consists of the overall results for the research work which has been done in this project. From the fabrication part to the PDMS templates process leading to successfully obtain PEG based and BCPs self-assembled patterns. All schemes and designs discussed in previous chapters are shown here with their final outcomes.

6.1 Results for SU-8 Templates

The result for the optimized masks created and discussed in chapter 3 and 4 are shown below in **Fig. 25 (a)**. While the PDMS mold of the same patterns are shown in **Fig. 25 (b)** which is made from soft lithography.

Fig. 25. a) Fabricated patterns on Silicon Wafer with 20u width and 100u Interspace

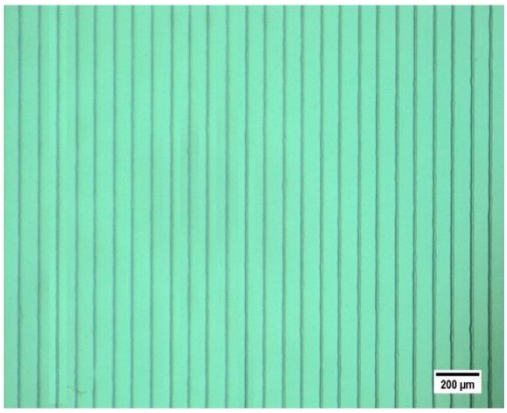

Fig 25. b) PDMS fabricated Molds for patterning BCPs

6.2 Results for NOA Templates

As explained earlier the fabrication process to get patterns from NOA UV sensitive glue, the results of these features are shown below. **Fig. 26 (a, b)** explicitly shows the fabricated patterns using photo-lithography on silicon wafers which further served as a template to obtain PDMS template to get NOA based negative replica of these desired features.

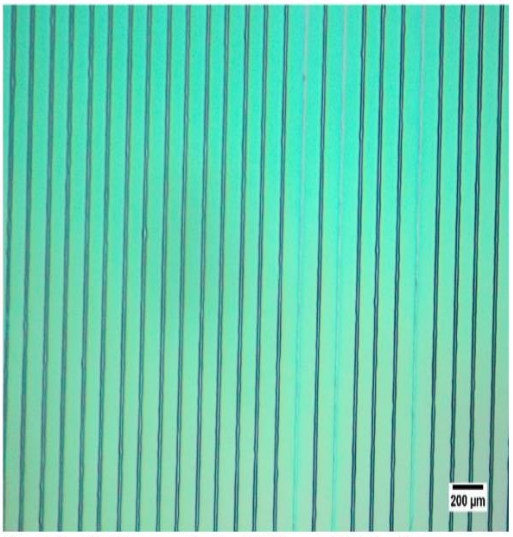

Fig. 26. a) Silicon wafer for NOA mold fabrication

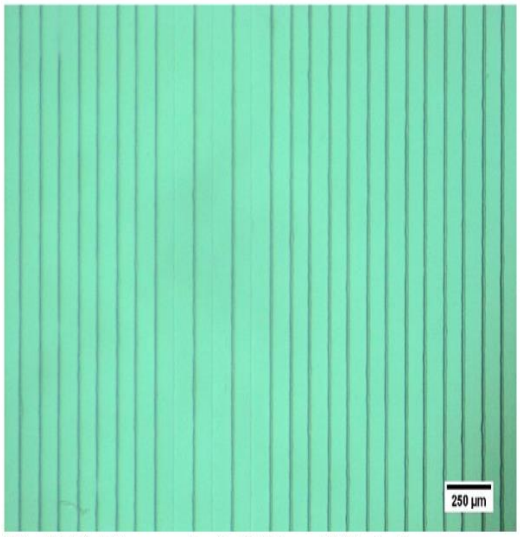

Fig. 26. b) Silicon wafer for NOA mold fabrication

6.3 Results for AFM Grid Templates

The patterns created by soft lithography of AFM grids are shown below in **Fig. 27**. Procedure of soft lithography is mentioned in detail already in chapter 4.

Results for CS AFM Calibration Standard Grid with bits and lines

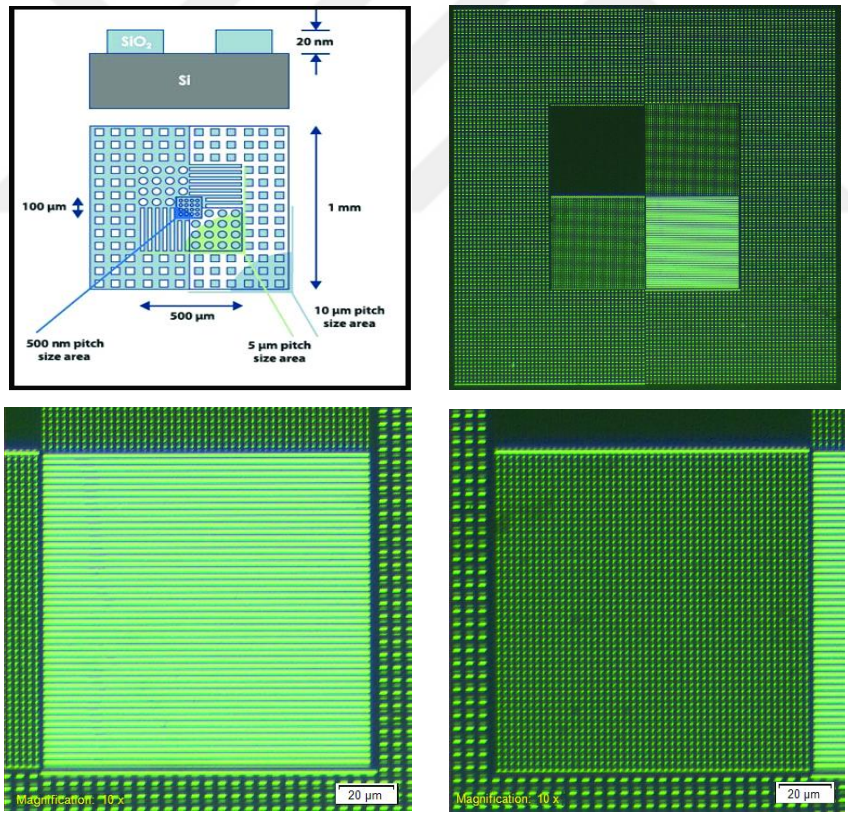

Fig. 27. a) Schematic of the CS AFM Grid and Fabricated PDMS molds of the AFM calibration grid with 500 µm x 500 µm chip size area

Results for TGZ3 AFM Calibration Grid with straight lines

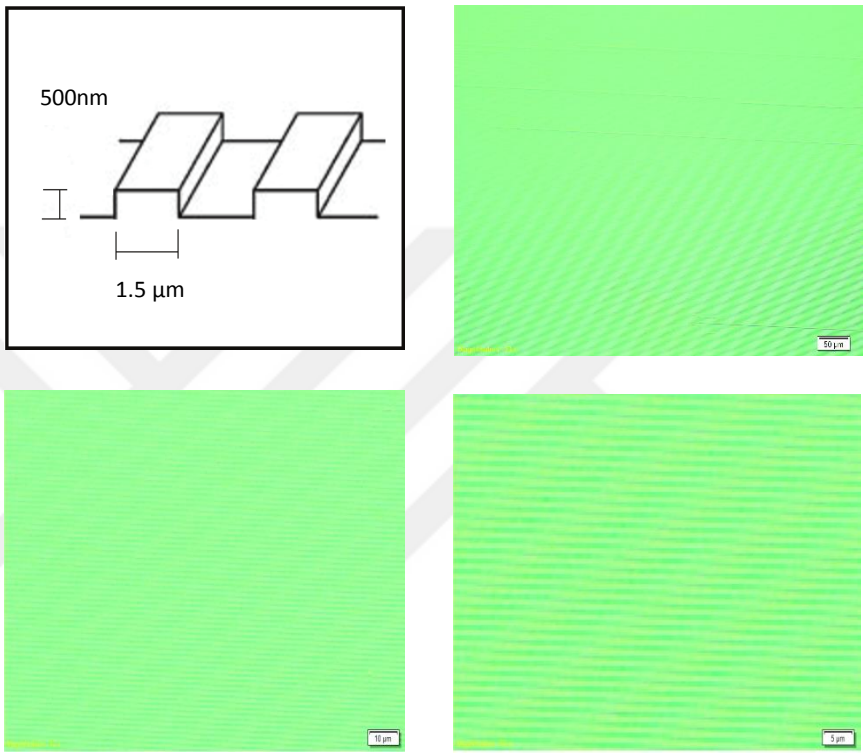

Fig. 28. Fabricated PDMS molds of the AFM calibration grid with 5 x 5 x 0.5mm chip size area

6.4 PEG-Based Polymer Formation Results

The schematic description of the process for fabricating arrays of NPs immobilized on patterns of polymer brushes prepared by MIMIC. The elastomeric molds were prepared by casting PDMS on top of the master substrates containing linear patterns of trenches using standard soft-lithography procedures. Placing the mold on top of a freshly cleaned silicon substrate resulted in open-ended channels sealed by the conformal contact enabled by the compliant nature of the PDMS. Organic solutions of polymers were spotted near the open end of the channels. We investigated polymers with two different backbone chemistries with identical end-functionality. Hydroxyl-terminated P2VP and PEG were dissolved in DMF and methanol, respectively. The latter polymer has hydroxyl groups at both ends of the polymer. The solutions filled the channels by capillary action and the mold was removed from the substrate following evaporation of the solvent. The resulting patterns of end-functional polymers were then subjected to a brief thermal annealing for grafting of the polymer chains to the substrate. Since the amount of deposited polymer is in excess of grafted chains, ungrafted polymer chains were removed by sonication in DMF and chloroform for P2VP and PEG, respectively. Patterns of polymer brushes then served as templates for guided attachment of colloidal gold nanoparticles which were immobilized by spotting a solution of Au NPs on the entire region followed by washing in water under sonication. The particles only attached to the patterned polymer brushes, thanks to the well-defined chemical patterning via MIMIC.

We employed two different types of master substrates to fabricate the PDMS molds. The master with the large features was fabricated by photolithography using a negative tone photoresist, whereas the other master consisted of a commercially available AFM grid **Fig. 29**. The master with the large features consisted of steps with the width of 20 µm, height of 10 µm and period of 100 µm. The grating patterns of the AFM grid had 1:1 ratio of the width to spacing with the width of 1.5 µm and height of ~500 nm. The patterns were fabricated with the specified dimension over large areas with the minimµm nµmber of defects. The surface of the master substrates was modified with 3-Aminopropy triethoxysilane before casting PDMS for easy separation of the mold from the substrate following curing. Note that the patterns in the mold are complementary to those on the master substrate; however, the patterns on the master are replicated on the surface of the target substrate following MIMIC.

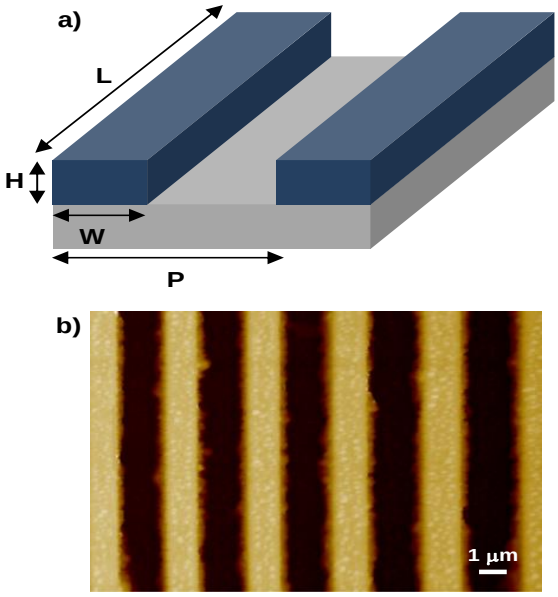

Fig. 29 Master substrates. **a)** Schematic description of the dimensions of the master substrates. For the master with the large features: L = 5 mm, H = 10 µm, W = 20 µm, P = 100 µm. For the AFM grid: L = 2 mm, H = 500 nm, W = 1.5 µm, P = 3 µm. **b)** AFM image of the master substrate consisting of the 1:1 grating patterns.

The complete filling of the channels formed by the mold and target substrate by the polymer solutions without loss of the conformal contact is the most critical aspect of patterning polymer brushes with the MIMIC process. Several factors including the surface energy of the channels, surface tension and viscosity of the solutions affect the filling the process [56]. Another important factor for organic solvents, is the swelling of the PDMS molds. Swelling not only can change the dimensions of the patterns, but also can destroy the conformal contact between the PDMS and target substrate.

We chose DMF and methanol which swell PDMS at low levels [57], for dissolving P2VP and PEG, respectively. Chlorobenzene used in spin-coating films of PEG, for example, led to immediate loss of the conformal contact of the mold with the substrate. Both polymer solutions completely filled the channels **Fig. 30 (a, c).** The complete filling of the channels with the polymer solutions can be explained by their wetting behavior of the silicon substrate and channels **Fig. 30 (b, d).** A solution of (1%) P2VP in DMF had a contact angle of 55^{o} on PDMS and $<10^{o}$ on silicon wafer. A solution of (1%) PEG in methanol had a contact angle of 22^{o} on PDMS and $<10^{o}$ on silicon wafer. Since the contact angles of the solutions on both the target and mold substrate is much less than 90^{o}, the filling of the channels are thermodynamically favorable [56]. Note that oxidizing PDMS molds by a plasma treatment can further decrease these contact angles; however, such process leads to the permanent bonding of the PDMS to the bare silicon wafer. The polymer solutions typically filled the channels at a rate of ~1.1 mm/s based on the relatively low molecular weight and therefore low viscosity of the solutions.

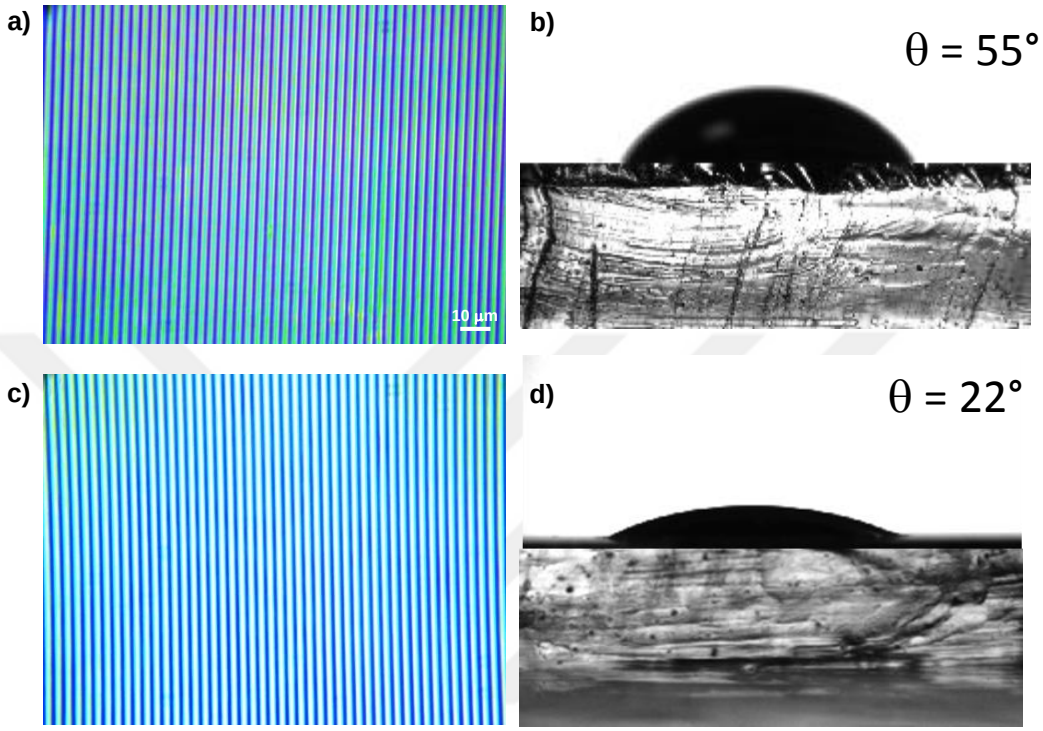

Fig. 30. Filling of the channels. **a, c)** Optical microscope images of the target substrates following the MIMIC process and removal of the PDMS mold for **a)** 1% P2VP-OH in DMF and **c)** 1% PEG in methanol. **b, d)** Images of droplets of **b)** 1% P2VP-OH in DMF and **d)** 1% PEG in methanol. The contact angle of the droplets are given at the top-right of the image.

The height profile of the patterns after MIMIC, annealing and washing steps inform about the localized grafting of brushes. We systematically characterized the height profile of the patterned samples after each step by AFM imaging. The images after each step were taken from the same region of the same substrates for consistency. **Fig. 31** presents the results for grafting P2VP and PEG brushes. The average height of the deposited patterns of end-functional polymers was above 200 nm after the MIMIC process. The edges of the patterns were slightly higher for the both polymers. Such edge effects are likely due to

transport of materials to the edge regions during the evaporation of the solvent with a phenomena known as the coffee-ring effect [58]. The width of the patterns was ~1.4 µm which was defined by the channels **Table 13**. The slightly lower width of the patterns in comparison to the width of the channels is probably a result of swelling and distortion of the PDMS molds during the MIMIC process. Thermal annealing of the patterns resulted in a certain level of spreading of the patterns with an increase in the width and decrease in the height of the patterns. Thermal annealing induced flow also led to a parabolic height profile with the maxima at the center of the pattern. PEG showed a slightly higher extent of spreading than P2VP, which could be related to the lower glass transition of the molecules. The removal of the excess and ungrafted material through washing resulted in grafted polymer chains with heights defined by the molecular weight of the polymers and grafting densities.

The height of the patterned polymer brushes was ~3.5 nm and ~10.0 nm for P2VP and PEG, respectively. These values are slightly lower than the thicknesses (~5.3 nm for P2VP, ~12.0 nm for PEG) obtained for brushes grafted in identical conditions from films deposited by spin-coating and correspond to grafting densities of 0.10 and 0.19 for P2VP and PEG brushes, respectively. The final patterns of grafted brushes has a roughness smaller than 1 nm. Irregularities in the center and edges of the patterns following the MIMIC process are not reflected to the patterns of brushes, since only chemically bound polymers remain attached to the substrate following the washing step. The width of the grafted brushes was typically lower than the width of the patterns following the thermal annealing **Fig. 31**. This interesting observation could be related to the presence of residual PDMS on the silicon in the regions where there was a contact between the mold and

substrate. Another factor could be the low heights of the patterns in the edge regions following the thermal annealing step.

Brush	Step	Width (μm)	Height (nm)
P2VP	After Mimic	1.33 ± 0.03	237.92 ± 11.48
	After Annealing	1.68 ± 0.03	215.31 ± 9.15
	After Washing	1.42 ± 0.04	3.50 ± 0.27
PEG	After Mimic	1.43 ± 0.03	218.67 ± 9.50
	After Annealing	1.94 ± 0.03	189.67 ± 6.80
	After Washing	1.70 ± 0.13	10.00 ± 0.65

Table 13. The width and height of the patterns after different steps.

Arrays of plasmonic NPs over large areas can be readily achieved on patterns of P2VP and PEG brushes prepared by the MIMIC process. Patterned P2VP and PEG brushes surrounded by silicon oxide serve as binding sites for the selective immobilization of citrate-stabilized Au NPs. SEM images presented in Figure 5 show that colloidal Au NPs attached to the patterns with a high level of specificity, i.e. the particles bound at high densities on the patterns with none or negligible binding to the background regions. The high level of specificity is a consequence of several factors: i) The MIMIC process enables additive patterning of materials without deposition of the materials to the background regions, thanks to the compliant nature of PDMS. ii) Citrate-stabilized Au NPs have a strong binding affinity towards P2VP and PEG brushes, allowing strong washing of the substrates under sonication following the immobilization of the particles. iii) The absence of interaction between the citrate-stabilized Au NPs and silicon oxide terminated background regions results in low levels of immobilized particles which are removed in the washing step.

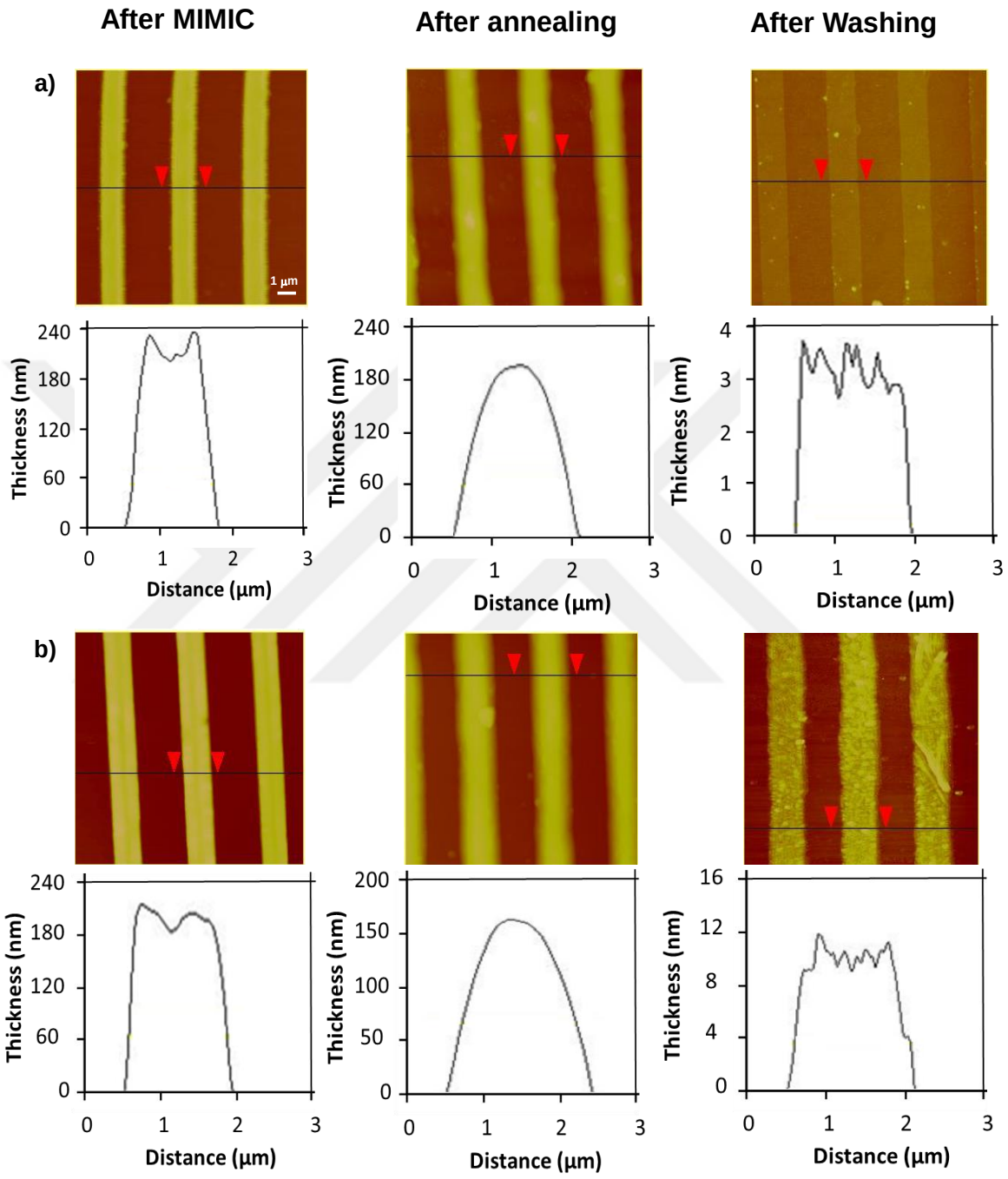

Fig. 31. Characterization of the height profiles of the patterns following the MIMIC process, grafting and washing steps. **a)** Grafting of P2VP brushes from 1% P2VP-OH in DMF and **b)** Grafting of PEG brushes from 1% PEG in methanol.

SEM images show in **Fig. 32**, that uniform arrays of particles could be obtained in widths defined by the mold. The use of molds with widths as small as several hundred nanometers could be possible based on the previously reported soft-lithography studies; however, several factors[59] such as incomplete filling and distortion in the patterns prevent from scaling down this process below 100 nm. We found that the nµmber of immobilized Au NPs was significantly higher on the patterned PEG brushes in comparison to homogenous PEG brushes deposited by spin-coating. The nµmber of immobilized Au NPs (20 nm in diameter) per square micrometer was 778 ± 11 and this nµmber reduced to 246 ± 8 particles on homogenous PEG brushes. This result is consistent with the previous study [55] where the density of bound particles on lithographically patterned PEG brushes was higher in comparison to homogenous substrates.

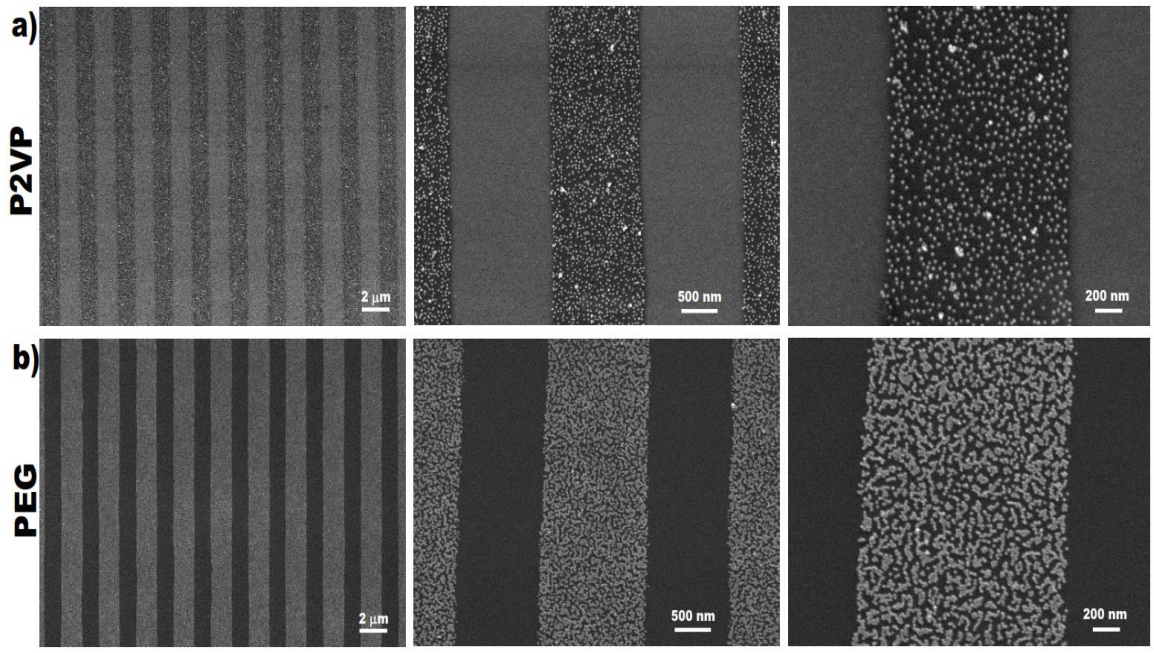

Fig. 32. SEM images of the NP arrays. **a)** P2VP and **b)** PEG brushes. The diameter of the particles is 20 nm.

It is likely that the kinetics of particle adsorption is enhanced by generating PEG brush grafted patterns surrounded by regions where there is no interaction with the Au NPs. The density of immobilized particles on patterned P2VP brushes, on the other hand, was 287 ± 7 NPs/μm^2 which is consistent with the values observed on homogenous PEG brushes deposited by spin-coating [60]. The contrast in the variance of the density of immobilized NPs between the patterned and homogeneous substrates for PEG and P2VP brushes probably relates to the different types of polymer-particle interaction.

6.5 BCPs Thin Films Formation Results

(1) 66,000-b-63,500 g / mol PS-b-PMMA

One of the most important parameters after solvent selection is the BCP concentration in the solution. The BCP concentration is important in determining the viscosity of the solution and determining the residual polymer thickness after evaporation in the canal. In the first experiments made, we used 0,025%, 0,25%, 1% and 2% BCP solids by weight. BCP was used with PS-b-PMMA having a molecular weight of 66,000-b-63,500 g / mol. The reason for the operation of the concentrating operation with this polymer is that the size and period of the structures which are formed according to the other polymers to be worked on are larger and the image is relatively easy to get.

6.5.1 BCP Formation using SU-8 Patterns and AFM Calibration Grids Patterns

(i) 0.025% PS-b-PMMA

In studies with channels with widths of 20 µms, it was seen that the channels were filled with BCP, but there was a change in color along the channel and therefore a change in thickness, as seen in the optical microscope pictures. FE-SEM studies have shown that the BCP structure is present in the channels. However, it has been observed that the nanostructures are not homogeneous across the entire channel area. Featureless portions in FE-SEM images often indicate cases where the orientations of the blocks are not perpendicular to the substrate surface. The same sample was also examined by SEM after FE-SEM etching with oxygen plasma. The build was not homogenous **Fig. 33**.

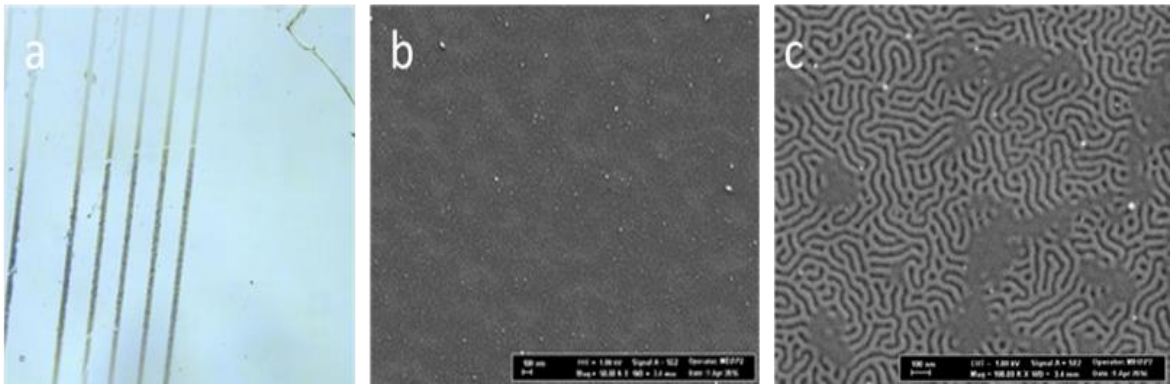

Fig. 33 a) 20 µm channels optical microscope image, **b-c)** Fe-SEM image at different magnifications

In studies with channels of width 1.5 µms, it was seen that the initial parts of the channels were filled with BCPs **Fig. 34**. Similar to the 20 µm channels, the nanostructures did not appear to be homogeneous.

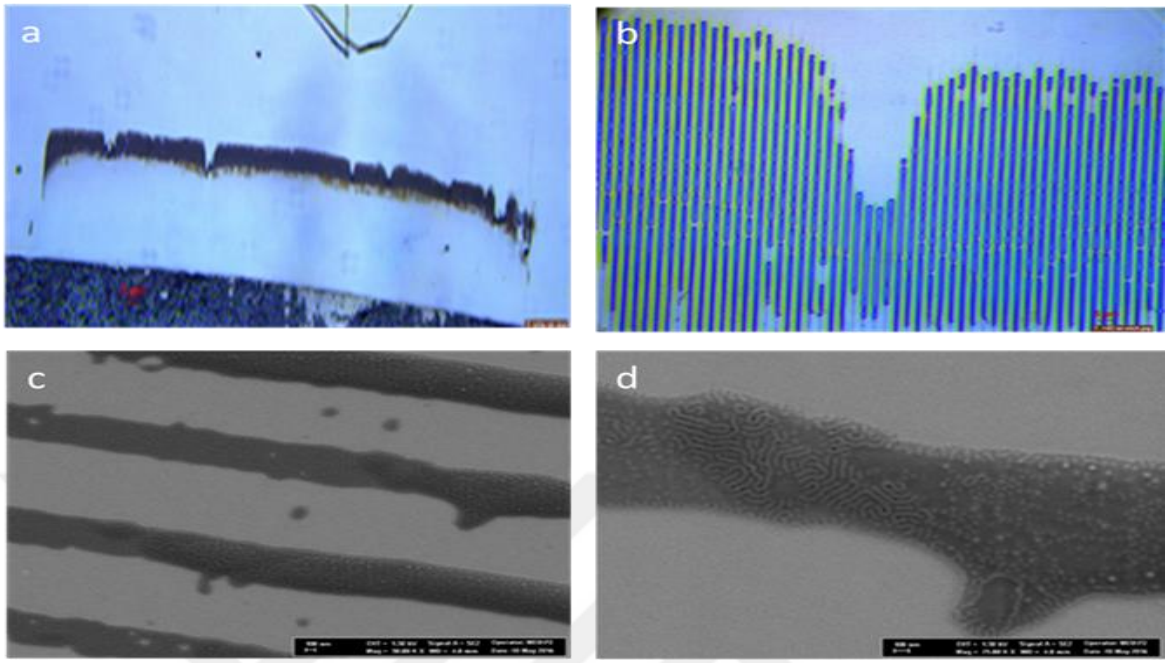

Fig. 34. % 0,025 PS-b-PMMA 66000-63500 g/mol DMF, Channels after 70 seconds of etching **a-b)** optical image, **c-d)** Fe-SEM image

(ii) 0.25% PS-b-PMMA

Studies with channels with widths of 20 µms have shown that BCP structures can form in large areas along the channels **Fig. 35**.

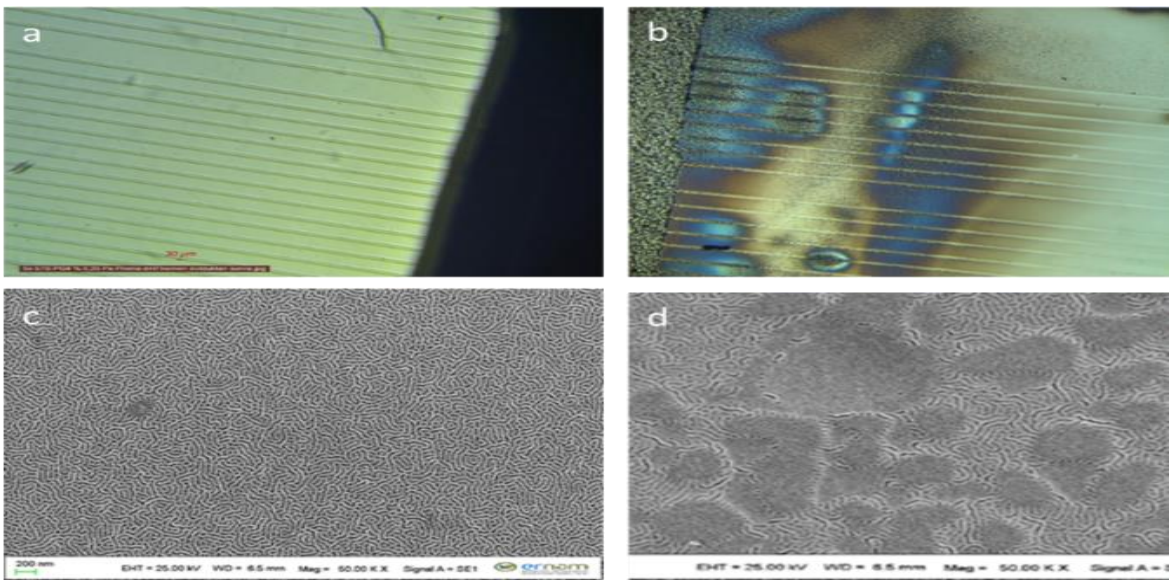

Fig. 35. 0,25% PS-b-PMMA on 57S-PG4 substrate 66000-63500 g / mol DMF **a)** During filling, **b)** after heating, **c-d)** after heating, SEM-20 µm channels at different amplitudes after heating.

(iii) % 1 PS-b-PMMA

Studies with channels with widths of 20 µms revealed that the BCP nanowires were formed in large quantities. In this BCP composition, further studies have been carried out on the control of solvent evaporation during the test. Experiments in a closed environment to slow the rate of evaporation have shown that BCP structures do not occur. It has been seen that the nanostructures can be formed homogeneously in studies made with channels with a width of 1.5 µms. It has been found that BCP structures are seen homogeneously in all of the linear patterns arranged one behind the other **Fig. 36**.

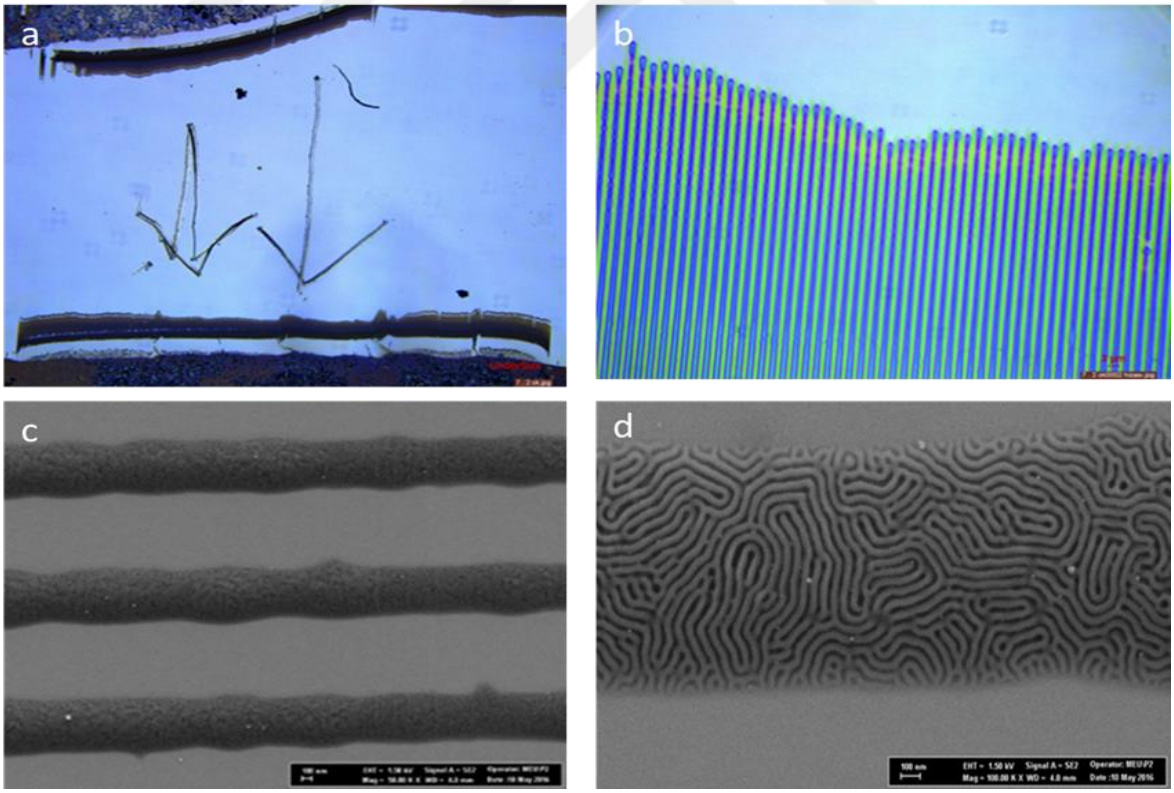

Fig. 36. Optical microscope image of 1% PS-b-PMMA 66000-63500 g / mol dmf **a-b) c-d)** Fe-SEM image at different magnification

(iv) % 2 PS-b-PMMA

When working with channels with a width of 1.5 µms, nanostructures could be formed homogeneously **Fig. 37.**

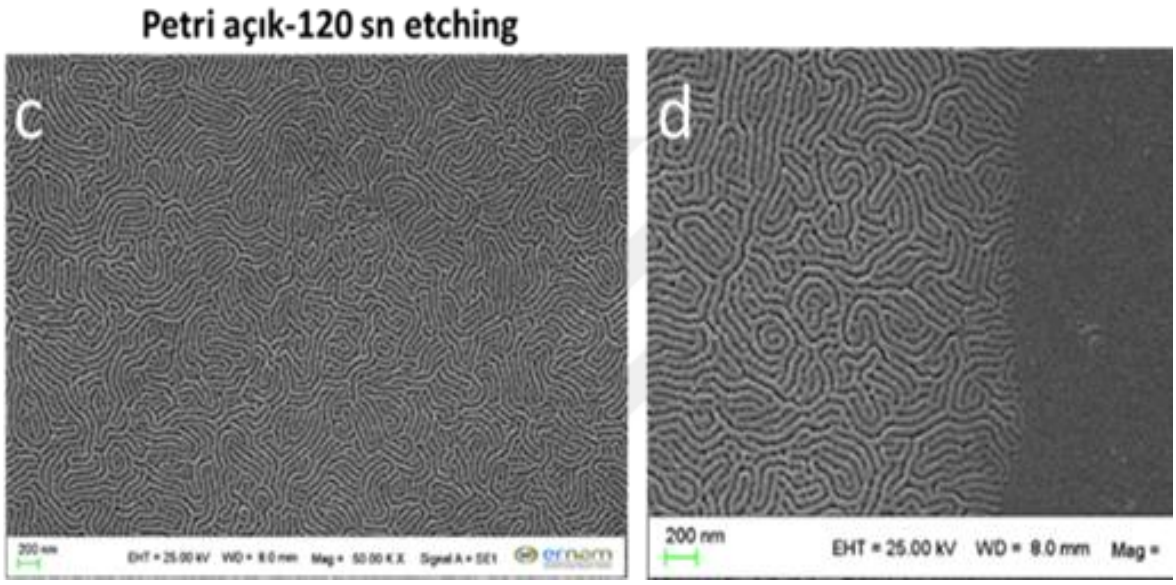

Fig. 37. 2 PS-b-PMMA 66000-63500 g/mol DMF Afm Grid c,d) SEM image

6.5.2 Characterization of BCP Films using different weights

Due to the good results in these conditions, AFM work has been carried out on these systems. The results shown in **Fig. 38**, show that nanostructures are formed and can be detected by AFM.

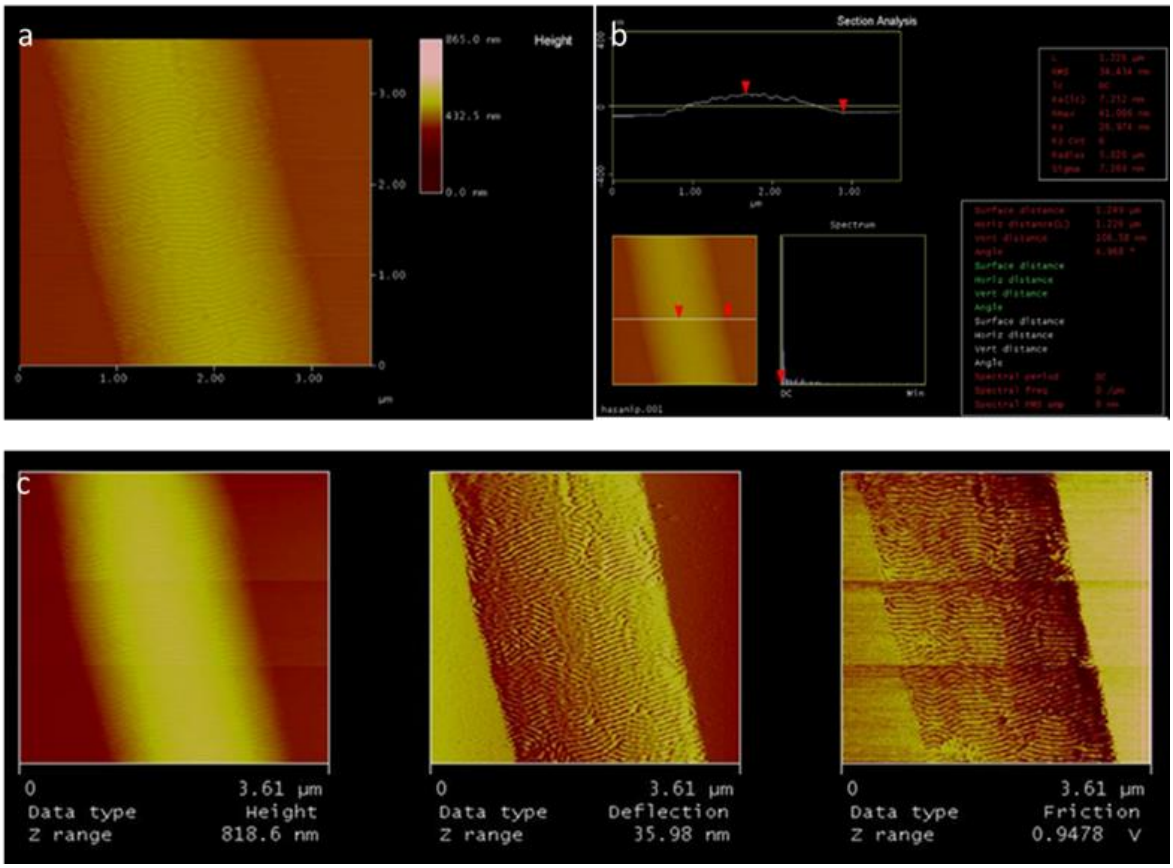

Fig. 38. 1% PS-b-PMMA from Au coating 66000-63500 AFM image a-c) the phase image of the channels, b) the post-mimic height of the channels (100 nm)

Deposition of BPCs on the surface with microfluidic dyes at different molecular weights

As stated in the project proposal, it is planned to work with PS-b-PMMA in four different molecular weights. These are PS-b-PMMA, which is distributed symmetrically in three blocks and forms a lamellar morphology. 66,000-b-63,500 g / mol, 37,000-b-37,000 g / mol

and 25,000-b-26,000 g / mol. Another polymer is PS-b-PMMA, which is rich in PS and has a cylindrical morphology of 46.100-b-21.000 g / mol. The use of BCPs in different molecular weights is aimed at creating nanowires of different size and morphology by self-regulation.

(2) 37,000-b-37,000 g / mol PS-b-PMMA

This polymer period with lamellar structure gives linear nanostructures of ~ 41 nm. This BCP has been studied to deposit on the surface with 1.5 μm wide channels. These structures have encountered a problem during the display of the PMMA block with a normal SEM with a metal coating following erosion with oxygen plasma. As can be seen in **Fig. 39**, many nanoparticles were found on the surface in SEM images. At the end of many experiments it has been found that these particles come from the coating made for SEM imaging. Experiments on the detection of this problem are given under a separate heading after this chapter.

As seen in **Fig. 40**, the BCP constructions seem to have been successful in the channels. There are particles on the surface with reduced coating time. Because the FE-SEM devices in Mersin and Bilecik were damaged, the first experiments with different molecular weights were performed with normal SEM.

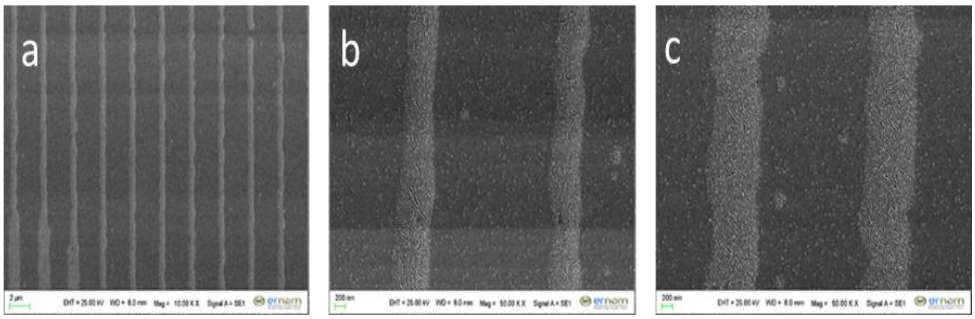

Fig. 39. SEM images Au coating (90 sec) 1% PS-b-PMMA 37000-37000 g / mol dmf-220 oC heating a-b-c) SEM images at different magnifications

(3) 25,000-b-26,000 g / mol PS-b-PMMA

This polymer period with lamellar structure gives linear nanostructures with ~ 27 nm. This BCP has been studied to deposit on the surface with 1.5 µm wide channels. Figures 23 and 24 show that this BCP can also be deposited on the surface with microfluidic channels and nanostructures are formed. In some samples **Fig. 41**, some defects were observed on the patterns. Due to the reasons explained above, the particle problem also appears in these experiments.

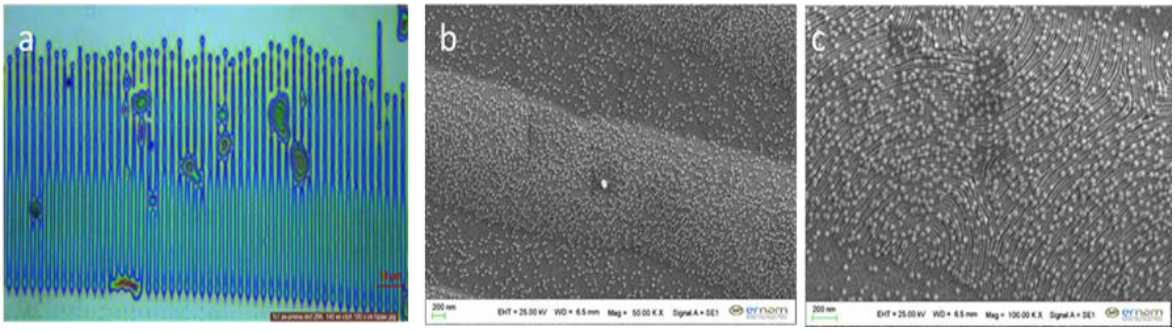

Fig. 40. SEM images Au coating (120 sec) 1% PS-b-PMMA 25000-26000 g / mol dmf-250 oC heating **a)** optics, **b-c)** SEM images

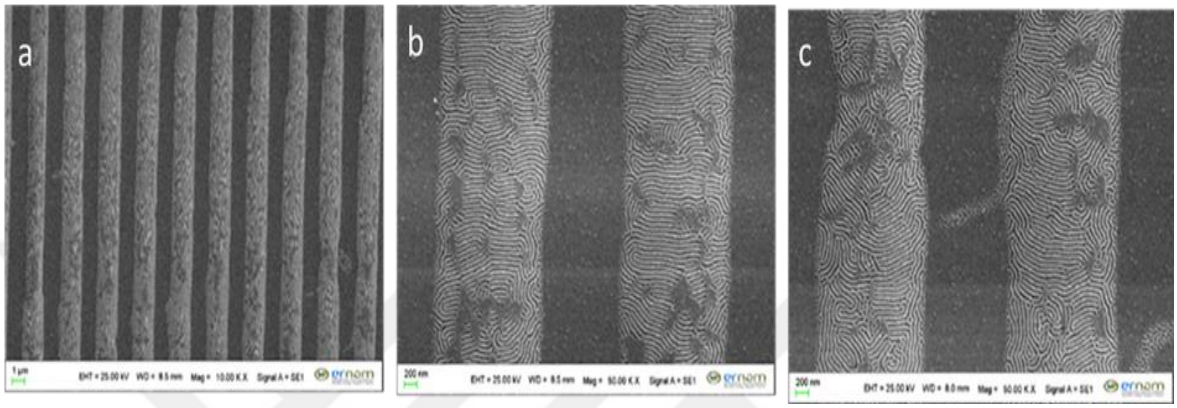

Fig. 41. SEM images Au coating (90 sec) **a)**1% PS-b-PMMA 25000-26000 g / mol dmf -220 oC heating a) optics, **b-c)** SEM images

We finally investigated the functionality and uniformity of the patterned gold nanoparticles by mapping the SERS response of the fabricated substrates. Localized suface plasmon resonances of metallic nanostructures result in electromagnetic enhancement of signals observed in Raman spectroscopy. Therefore mapping the characteristic peak of a reporter molecule in Raman spectroscopy directly informs about the functionality and uniformity of the fabricated NP arrays. Figure 6 summarizes SERS results on the arrays of NPs generated on patterns of P2VP and PEG brushes using rhodamine 6G as the reporter molecule. The mapping of the peak at a position of 1361 cm-1 shows specific and strong signals are received from the patterns where Au NPs are located. An interesting result is that the intensity of signals was higher for NPs immobilized on the patterned brushes in comparison to homogenous brushes prepared by spin-coating (Figure 6.c). Two factors

contribute to such enhancement of the signals. First, the density of particles per unit area is larger in the case of patterned brushes, resulting in higher density of scattering centers. Second, the placement of NPs in close-proximity results in areas where electromagnetic fields are focused in small gaps called as hot-spots. The mapping of the SERS response also inform about the uniformity of the density of the bound particles over areas that are much larger than that can be observed by SEM imaging. The intensity of the signals from the patterns was mostly uniform; however, some of the lines had regions of weak SERS response. We found out that the density of particles in these defective regions are lower than the rest of the patterns. These defective regions were typically less than 10% of the total area and probably formed as a result of issues during the MIMIC process such as contaminations from the PDMS molds.

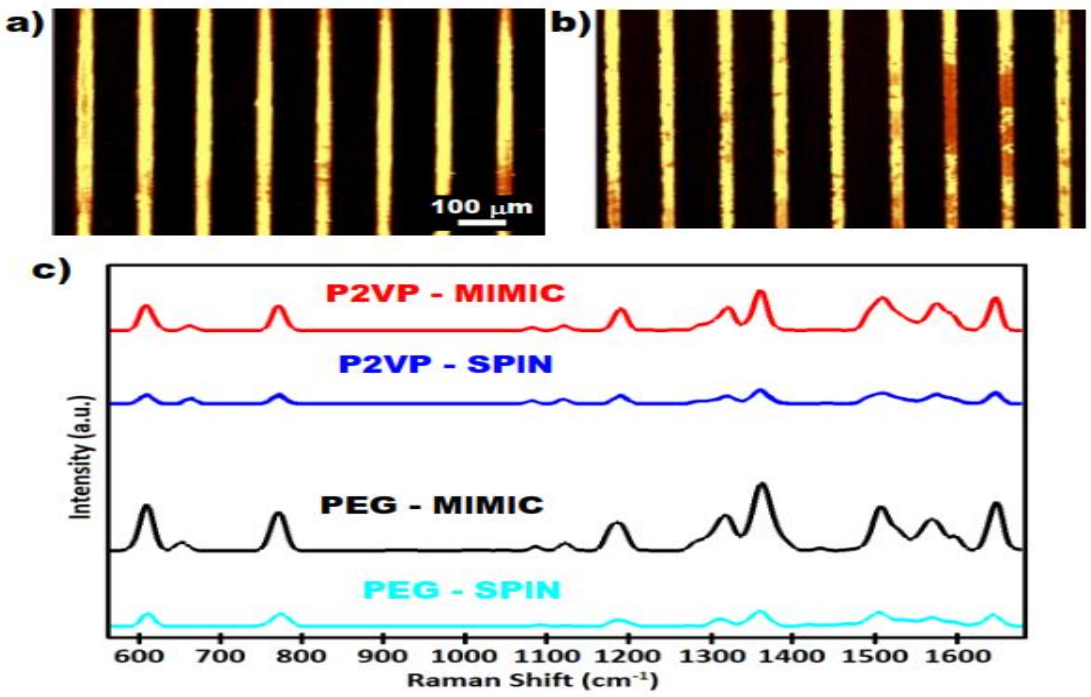

Figure 6. SERS results on the patterned P2VP and PEG brushes. Raman mapping of rhodamine 6G on patterns of a) P2VP and b) PEG brushes. c) Raman scattering spectra of rhodamine 6G on immobilized particles. The diameter of the particles is 60 nm.

CONCLUSSION

A soft lithographic approach relying on capillary flow of solutions is used to fabricate patterns of polymers on large surface areas not only from the self-assembly attribute of block copolymers (BCPs), but also to form polymers using end-functional P2VP and PEG molecules. This approach enables low-cost, large area patterning of polymer films. This inexpensive method to pattern large areas using BCP self-assembly through elastomeric PDMS molds would give boost to the solution of the commercialization of nano-patterns below ~20nm for semiconductor industries with an explicit ease of fabrication. While for polymer brushes, the lateral dimensions of the patterns are defined by the mold, whereas the height of the resulting brushes are determined by the grafting process as a function of the chain length and grafting length. The ability to pattern end-grafted polymer chains P2VP and PEG with a high level of specificity allowed for fabrication of patterned assemblies of plasmonic NPs which show strong SERS effects. This platform can serve as foundation for advanced sensor systems through integration of multiple analyte molecules on the plasmonic NPs using microfluidic channels. The backbone chemistry of the patterned polymers as well as colloidal NPs can be varied according to the needs of specific applications.

REFERENCES

[1] Sheng-Li Lu, Mu-Jie Yang, and Feng-Lian Bai. Synthesis, electrochemical, and optical properties of a novel PPV/PPE block-copolymer. Macromolecular Rapid Communications, 25(9):968–971, May 2004.

[2] Stephan Forster and Markus Antonietti. Amphiphilic block copolymers in structure-controlled nanomaterial hybrids. Advanced Materials, 10:195–217, February 1998.

[3] Business and industry review encyclopedia Britannica. From encyclopedia Britannica online. http://www.search.eb.com/eb/article?tocid=231753

[4] W. Kuhn. Beiziehungen zwischen Molekulgrosse, statistischer Molekugestaltund elastischen Eigenschaften hochpolymerer Stoff e. Kolloid Zeitschrift, 76:258, 1936.

[5] W. Kuhn. Molekulkonstellation und Kristallitorientierung als Ursachen kautschukahnlicher Elastizitat. Kolloid Zeitschrift, 87:3, 1939.

[6] Johan T. Padding, *THEORY OF POLYMER DYNAMICS*, Theoretical Chemistry, University of Cambridge, United Kingdom

[7] Raymond F. Boyer. The relation of transition temperatures to chemical structure in high polymers. Rubber Chemistry and Technology, 36(5):1303, 1963

[8] Structural studies of block copolymers and block copolymer / alμminosilicate materials "A dissertation by G. E. S. Toombes, August 2007.

[9] Segalman, Rachel A. "Patterning with block copolymer thin films." *Materials Science and Engineering: R: Reports* 48.6 (2005): 191-226.

[10] Wu, Mei-Ling, Dong Wang, and Li-Jun Wan. "Directed block copolymer self-assembly implemented via surface-embedded electrets." *Nature communications* 7 (2016).

[11] L. F. Thompson, C. G. Willson, and M. J. Bowden, Introduction to Microlithography. Washington, DC: Oxford Univ. Press, 1983.

[12] H. J. Levinson, Principles of Lithography, vol. PM146, 2nd ed. Bellingham, WA: SPIE.

[13] S. Owa, H. Nagasaka, K. Nakano, and Y. Ohmura, Current status and future prospect of immersion lithography, Proc. SPIE, 2006, vol. 6154, 61 5408-1.

[14] H. Sewell, J. Mulkens, D. McCafferty, L. Markoya, B. Streefkerk, and P. Graeupner, The next phase for immersion lithography, in Proc. SPIE, vol. 6154, D. G. Flageilo, Ed., 2006, Optical Microlithography XIX, paper 615 406-1.

[15] M. D. Levenson, N. S. Viswanathan, and R. A. Simpson, Improving resolution in photolithography with a phase-shifting mask, IEEE Trans. Electron Devices, vol. ED-29, pp. 1828–1836, 1982.

[16] M. Shibuya, Projection master for transmitted illμmination, Japanese Patent Showa 62-50811, Oct. 27, 1987.

[17] D. C. Flanders and H. I. Smith, Spatial period division exposing, U.S. Patent 4 360 586, Apr. 14, 1980.

[18] D. R. Herriott et al., EBES, a practical electron lithographic system, IEEE Trans. Electron Devices, vol. 21, pp. 385–392, Jul. 1975.

[19] Pease, R. Fabian, and Stephen Y. Chou. "Lithography and other patterning techniques for future electronics." Proceedings of the IEEE 96.2 (2008): 248-270.

[20] J. Warlaμmont, X-ray lithography; on the road to manufacture,[J. Vac. Sci. Technol., vol. B7, pp. 2934–2938, 1989.

[21] S. Y. Chou, P. R. Krauss, and P. J. Renstrom, Imprint of sub-25 Nm vias and trenches in polymers, Appl. Phys. Lett., vol. 67, no. 21, pp. 3114–3116, 1995.

[22] Guo, L. Jay. "Nanoimprint lithography: methods and material requirements." Advanced Materials 19.4 (2007): 495-513.

[23] B. D. Gates et al., New approaches to nanofabrication: Molding, printing, and techniques, Chem. Rev., vol. 105, no. 4, pp. 1171–1196, 2005

[24] J. Y. Cheng et al., Templated self-assembly of block copolymers: Effect of substrate topography, Adv. Mater., vol. 15, no. 19, p. 1599, 2003.

[25] C. T. Black and O. Bezencenet, Nanometer-scale pattern registration and alignment by directed diblock copolymer self-assembly, [IEEE Trans. Nanotechnol., vol. 3, pp. 412–415, Sep. 2004.

[26] C. T. Black, Self-aligned self-assembly of multi-nanowire silicon field effect transistors, Appl. Phys. Lett., vol. 87, no. 16, p. 163 116, 2005.

[27] M. P. Stoykovich, M. Muller, S. O. Kim et al., Directed assembly of block copolymer blends into nonregular device-oriented structures, Science, vol. 308, no. 5727, pp. 1442–1446, 2005.

[28] International Technology Roadmap for Semıconductors 2013 Edition, LITHOGRAPHY

[29] International Technology Roadmap for Semıconductors 2013 Edition, Emerging Research Materials (EMR)

[30] ITRS lithography roadmap: 2015 challenges

[31] Pimpin, Alongkorn, and Werayut Srituravanich. "Review on micro-and nanolithography techniques and their applications." Engineering Journal 16.1 (2011): 37-56.

[32] M. J. Madou, Fundamentals of Microfabrication: The Science of Miniaturization, 2nd ed. New York: CRC, 2002.

[33] B. D. Gates, Q. Xu, M. Stewart, D. Ryan, C. G. Willson, and G. M. Whitesides, "New approaches to nanofabrication: Molding, printing, and other techniques," Chem. Rev., vol. 105, pp. 1171-96, 2005.

[34] R. F. Pease and S. Y. Chou, "Lithography and other patterning techniques for future electronics," Proc. IEEE, vol. 96, pp. 248-270, 2008.

[35] R. Menon, A. Patel, D. Gil, and H. I. Smith, "Maskless lithography," Mater. Today, vol. 8, pp. 26-33, 2005.

[36] M. Altissimo, "E-beam lithography for micro-/nanofabrication," Biomicrofluidics, vol. 4, pp. 36, 2010.

[37] W. Shim, A. B. Braunschweig, X. Liao, J. Chai, J. K. Lim, G. F. Zheng, and C. A. Mirkin, "Hard-tip, Soft-spring Lithography," Nature, vol. 469, pp. 516-520, 2011.

[38] D. Roy, M. Munz, P. Colombi, S. Bhattacharyya, J-P. Salvetat, P. J. Cµmpson, and M. L. Saboungi, "Directly writing with nanoparticles at the nanoscale using dip-pen nanolithography," Appl. Surf. Sci., vol. 254, pp. 1394-1398, 2007.

[39] B. Li, Y. Zhang, J. Hu, and M. Li, "Fabricating protein nanopatterns on a single DNA molecule with Dip-pen nanolithography," Ultramicroscopy, vol. 105, pp. 312-315, 2005.

[40] Q. Tang and S-Q. Shi, "Preparation of gas sensors via dip-pen nanolithography," Sens. Actuators B, vol. 131, pp. 379-383, 2008.

[41] S. Y. Chou, P. R. Krauss, and P. J. Renstrom, "Imprint lithography with 25 –nanometer resolution," Science, vol. 272, pp. 85-87, 1996.

[42] S. Y. Chou, P. R. Krauss, "Imprint lithography with sub-10nm feature size and high throughput," Microelectronic Eng., vol. 35, pp. 237-240, 1997.

[43] A. Cattoni, E. Cambril, D. Decanini, G. Faini, and A. M. Haghiri-Gosnet, “Soft UV-NIL at 20 nm scale using flexible bi-layer stamp casted on HSQ master mold,” Microelectron. Eng., vol. 87, pp. 1015-1018, 2010.

[44] J. Chen, J. Shi, D. Decanini, E. Cambril, Y. Chen, and A. M. Haghiri-Gosnet, “Gold nanohole arrays for biochemical sensing fabricated by soft UV nanoimprint lithography,” Microelectron. Eng., vol. 86, pp. 632-635, 2009.

[45] C. F. Cooper, “George Whitesides: Molecular self-assembly and the invention of soft lithography,” J. Franklin Inst., vol. 348, pp. 544-554, 2011.

[46] Timothy P. Lodge “Block Copolymers: Past Successes and Future Challenges”, Macromol. Chem. Phys. 2003, 204, 265–273

[47] F. S. Bates, G. H. Fredrickson, Block Copolymers—Designer Soft Materials Phys. Today 1999, 52, 32.

[48] Ruiz, Ricardo, et al. "Density multiplication and improved lithography by directed block copolymer assembly." Science 321.5891 (2008): 936-939.

[49] Radha, B., and G. U. Kulkarni. "Dewetting assisted patterning of polystyrene by soft lithography to create nanotrenches for nanomaterial deposition." ACS applied materials & interfaces 1.2 (2009): 257-260.

[50] Onses, M. Serdar, et al. "Hierarchical patterns of three-dimensional block-copolymer films formed by electrohydrodynamic jet printing and self-assembly." Nature nanotechnology 8.9 (2013): 667-675.

[51] NOA details: https://www.thorlabs.com/newgrouppage9.cfm?objectgroup_id=196

[52] TGZ3 AFM Calibration Grid details:
https://www.tedpella.com/calibration_html/AFM_SPM_Calibration.htm#HS20MG

[53] CS AFM Calibration Grid:
https://www.tedpella.com/calibration_html/AFM_SPM_Calibration.htm#HS20MG

[54] Kim, Enoch, Younan Xia, and George M. Whitesides. "Micromolding in capillaries: applications in materials science." *Journal of the American Chemical Society* 118.24 (1996): 5722-5731.

[55] M.S. Onses, P.F. Nealey, Tunable Assembly of Gold Nanoparticles on Nanopatterned Poly(ethylene glycol) Brushes, Small, 9 (2013) 4168-4174.

[56] E. Kim, Y.N. Xia, G.M. Whitesides, Micromolding in capillaries: Applications in materials science, J Am Chem Soc, 118 (1996) 5722-5731.

[57] J.N. Lee, C. Park, G.M. Whitesides, Solvent compatibility of poly(dimethylsiloxane)-based microfluidic devices, Anal Chem, 75 (2003) 6544-6554.

[58] P.J. Yunker, T. Still, M.A. Lohr, A.G. Yodh, Suppression of the coffee-ring effect by shapedependent capillary interactions, Nature, 476 (2011) 308-311.

[59] Y.N. Xia, G.M. Whitesides, Soft lithography, Angew Chem Int Edit, 37 (1998) 550-575.

[60] H. Yilmaz, S. Pekdemir, H.H. Ipekci, N.B. Kiremitler, M. Hancer, M.S. Onses, Ambient, rapid and facile deposition of polymer brushes for immobilization of plasmonic nanoparticles, Appl Surf Sci, 385 (2016) 299-307.